AD-A075 146 VANDERBILT UNIV NASHVILLE TN DEPT OF PHYSICS AND AST--ETC F/G 20/3
APPLICATION OF SENSITIVITY VECTORS TO THE MEASUREMENT AND MODEL--ETC(U)
SEP 79 J P WIKSWO N00167-77-M-8018

UNCLASSIFIED DTNSRDC/PAS-79/1 NL

| OF |

AD
A075146

END
DATE
FILMED
11 -79
DDC

1.0 4.5 5.0 5.6 6.3 7.1 8.0 9.0 2.8 3.2 3.6 4.0 2.5 2.2 2.0

1.1 1.8

1.25 1.4 1.6

MICROCOPY RESOLUTION TEST CHART

NATIONAL BUREAU OF STANDARDS-1963-A

6

DAVID W. TAYLOR NAVAL SHIP RESEARCH AND DEVELOPMENT CENTER

Bethesda, Maryland 20084

LEVEL II

APPLICATION OF SENSITIVITY VECTORS TO THE MEASUREMENT AND MODELLING OF MAGNETOSTATIC FIELDS

By
John P. Wikswo, Jr.

APPROVED FOR PUBLIC RELEASE: DISTRIBUTION UNLIMITED

PROPULSION AND AUXILIARY SYSTEMS DEPARTMENT
RESEARCH AND DEVELOPMENT REPORT

September 1979 DTNSRDC/PAS-79-1

DTNSRDC/PAS-79-1

APPLICATION OF SENSITIVITY VECTORS TO THE MEASUREMENT AND MODELLING OF MAGNETOSTATIC FIELDS

MAJOR DTNSRDC ORGANIZATIONAL COMPONENTS

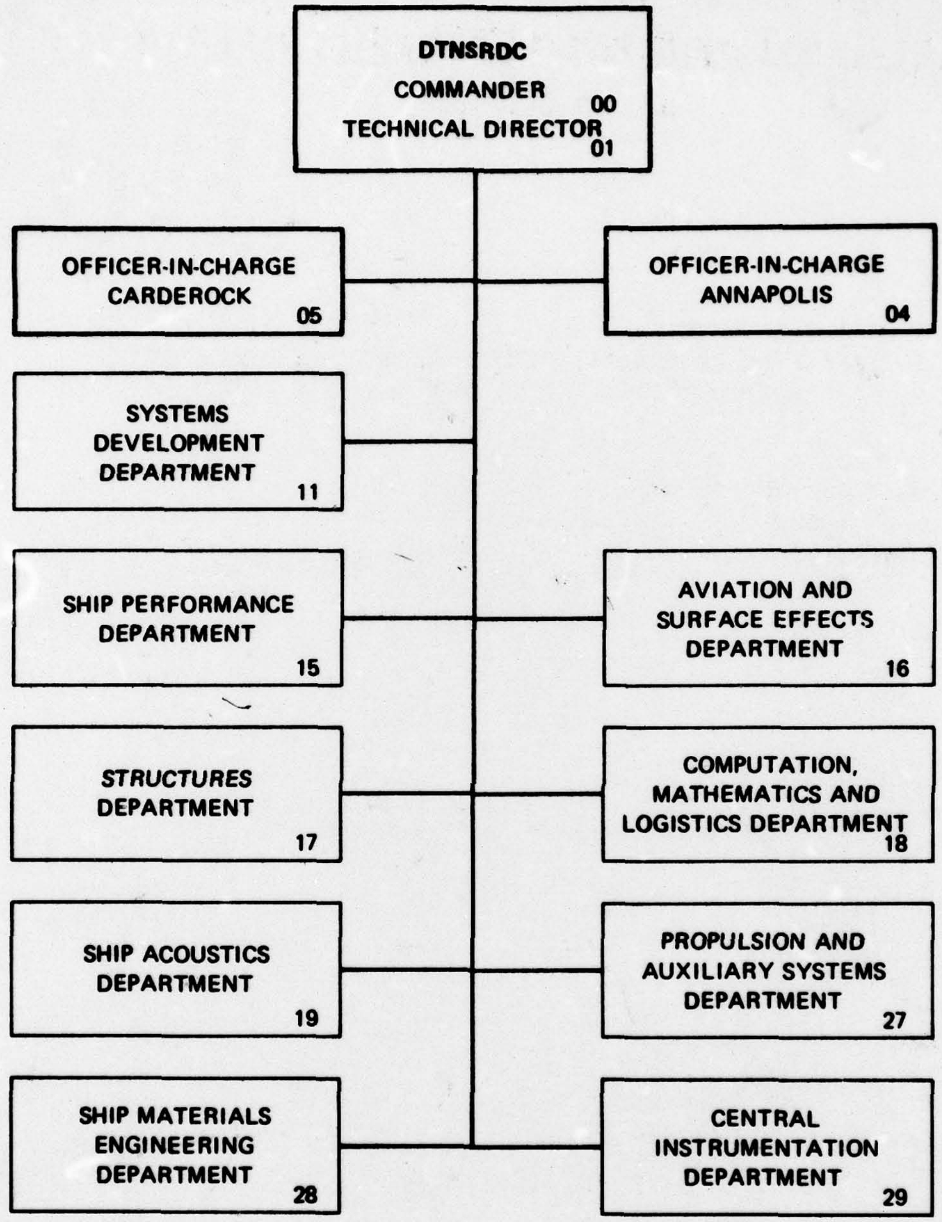

NDW-DTNSRDC 3960/43b (Rev. 3-78)
GPO 928 740

UNCLASSIFIED

SECURITY CLASSIFICATION OF THIS PAGE (When Data Entered)

REPORT DOCUMENTATION PAGE		READ INSTRUCTIONS BEFORE COMPLETING FORM
1. REPORT NUMBER 18 DTNSRDC/PAS[redacted]	2. GOVT ACCESSION NO. 19 79/7	3. RECIPIENT'S CATALOG NUMBER
4. TITLE (and Subtitle) 6 Application of Sensitivity Vectors to the Measurement and Modelling of Magnetostatic Fields.		5. TYPE OF REPORT & PERIOD COVERED
		6. PERFORMING ORG. REPORT NUMBER
7. AUTHOR(s) 10 John P. Wikswo, Jr		8. CONTRACT OR GRANT NUMBER(s) 15 N00167-77-M-8018 new
9. PERFORMING ORGANIZATION NAME AND ADDRESS S/C Department of Physics and Astronomy Vanderbilt University, Box 1807, Station B Nashville, Tenn. 37235		10. PROGRAM ELEMENT, PROJECT, TASK AREA & WORK UNIT NUMBERS B0005-SL 001, PE 11221N, 2704-110
11. CONTROLLING OFFICE NAME AND ADDRESS David W. Taylor Naval Ship Research and Development Center, Annapolis, Maryland 21402		12. REPORT DATE 11 Sep[redacted]79
		13. NUMBER OF PAGES 71 pages
14. MONITORING AGENCY NAME & ADDRESS (if different from Controlling Office) The Naval Material Command (PM-2) (Project Manager) 12 80		15. SECURITY CLASS. (of this report) Unclassified
		15a. DECLASSIFICATION/DOWNGRADING SCHEDULE

16. DISTRIBUTION STATEMENT (of this Report)

Approved for Public Release: Distribution Unlimited

17. DISTRIBUTION STATEMENT (of the abstract entered in Block 20, if different from Report)

9 **Research and development rept.,**

18. SUPPLEMENTARY NOTES

19. KEY WORDS (Continue on reverse side if necessary and identify by block number)

Magnetostatic Fields
Sensitivity Vectors
Magnetic Field Measurements

20. ABSTRACT (Continue on reverse side if necessary and identify by block number)

The purpose of this report is to develop the analytic techniques required for quantitative assessment of the sensitivity of magnetic field measurements to quasi-static magnetic sources. To do this, we first use the concept of the gradient vector to define a "sensitivity vector" for a given field measurement, and then relate this vector to the results obtained from the reciprocity theorem of electromagnetism. The derivations are then extended from magnetic dipoles to higher order moments. Several non-linear cases are examined, and techniques are developed to account for the presence of noise.

DD FORM 1 JAN 73 1473 EDITION OF 1 NOV 65 IS OBSOLETE

S/N 0102-LF-014-6601

UNCLASSIFIED 401 892

SECURITY CLASSIFICATION OF THIS PAGE (When Data Entered)

TABLE OF CONTENTS

EXECUTIVE SUMMARY

APPLICATION OF SENSITIVITY VECTORS TO THE MEASUREMENT AND MODELLING OF MAGNETOSTATIC FIELDS

OBJECTIVE

The objective of this report is to develop the analytic techniques required for quantitative assessment of the sensitivity of magnetic field measurements to quasi-static magnetic sources.

APPROACH

To accomplish this objective we first use the concept of the gradient vector to define a "sensitivity vector" for a given field measurement, and then relate this vector to the results obtained from the reciprocity theorem of electromagnetism. The derivations will then be extended from magnetic dipoles to higher order moments. Several non-linear cases will be examined, and techniques will be developed to account for the presence of noise.

RESULTS

In this report, the mathematical basis of sensitivity vectors has been developed, with specific application to the measurement and modelling of magnetic fields. In the course of analyzing several examples, the following questions were answered:

1. Given two magnetic field measurements, what criteria must be satisfied to allow determination of the two dipole components consistent with that field?

2. For a measurement of the vector magnetic field at a fixed distance from a dipole source, what is the optimum magnetometer position?

3. How do various configurations of single axis magnetometers compare in terms of their ability to determine model parameters, and how can this be assessed quantitatively?

4. How can the presence of noise be included in such an analysis?

5. What is the relationship of the sensitivity vector concept to the reciprocity theorem of electromagnetic fields?

6. How can sensitivity vectors be used to study multipole models?

7. What is the interpretation of a sensitivity vector for a non-linear model?

8. What is the position dependence of a vector magnetometer, and how does it vary with position?

9. Where can a magnetometer be placed relative to the model to insure adequate signal to noise ratio?

Based on the ability of the sensitivity vector approach to answer these questions quantitatively, it appears that this type of analysis may be valuable for optimizing magnetometer array configurations. It is reassuring that the results obtained in this report are consistent with both a modeller's intuition and more abstract mathematical analysis, particularly in that this method can be readily extended to more complicated systems where intuition fails.

RECOMMENDATIONS

Two specific recommendations follow from these results:

1) Interactive computer code should be developed to allow accurate and rapid analysis of magnetometer sensitivity and comparison of magnetometer configurations.

2) The sensitivity vector analysis should be extended to include the magnetic field from electric current distributions, and possibly the electric field from these currents.

I. INTRODUCTION

The purpose of this report is to develop the analytic techniques required for quantitative assessment of the sensitivity of magnetic field measurements to quasi-static magnetic sources. To do this, we will first use the concept of the gradient vector to define a "sensitivity vector" for a given field measurement, and then relate this vector to the results obtained from the reciprocity theorem of electromagnetism. The derivations will then be extended from magnetic dipoles to higher order moments. Several non-linear cases will be examined, and techniques will be developed to account for the presence of noise.

II. THE CONCEPT OF A SENSITIVITY VECTOR

Let us consider an object that is a source of electric and magnetic fields. We are able to make electromagnetic measurements at some distance from the object, and wish to use these measurements to obtain a mathematical description of the field sources. We can accomplish this by defining a hypothetical model for the sources and by adjusting various model parameters until the fields produced by the model match the observed ones. In practice, this process is complicated by linear dependence of various model parameters for a particular set of measurements, by the presence of noise in the measured data, and by the inability of the model to explain certain details of the fields. The last one of these complications can be remedied only by altering the model and will not be considered in this report. The first two, linear dependence and noise, can be addressed using sensitivity vectors.

We will treat each measurement as a scalar*. Measurement of a vector magnetic field is equivalent to three single axis field measurements that determine three orthogonal vector components. Other scalars that we might measure are the component of the magnetic field parallel to the earth's geomagnetic field, $\frac{\vec{B} \cdot \vec{B}_{earth}}{|\vec{B}_{earth}|}$, the field magnitude $|\vec{B}|$, or electric field components E_i and magnitude $|\vec{E}|$. In general, we will make field measurements F_i at points $\vec{r}_i$. An arbitrary number of different measurements can be made at a single point, in which case $F_i = F_j$ but $\vec{r}_i = \vec{r}_j$. The process of modelling involves using these measurements to specify the parameters of a model which reproduces the fields to the desired accuracy. Suppose the model is located at $\vec{r}'$ and is specified by n model parameters M_j. As an example, a magnetic dipole model at a known location has three

*i.e., a scalar quantity as opposed to a vector quantity, not to be confused with a total field magnetometer.

parameters $M_1 = m_x$, $M_2 = m_y$ and $M_3 = m_z$. Addition of a quadrupole adds five more parameters to the model.

If m measurements F_i are made to determine the n parameters M_j, we can say that the field or measurement space has n dimensions while the source or model space has m dimensions. If the F's and M's are linearly related, we can write

$$\begin{pmatrix} F_1 \\ \cdot \\ \cdot \\ F_N \end{pmatrix} = \begin{pmatrix} T_1 & \cdots\cdots & T_{1M} \\ \cdot & \cdot & \cdot \\ \cdot & \cdot & \cdot \\ T_{N1} & \cdots\cdots & T_{NM} \end{pmatrix} \begin{pmatrix} M_1 \\ \cdot \\ \cdot \\ M_M \end{pmatrix} \tag{2.1}$$

which in matrix notation is

$$\tilde{F} = \tilde{T}\,\tilde{M} \tag{2.2}$$

where $\tilde{F}$ is a n x 1 matrix; $\tilde{M}$ is a m x 1 matrix, and $\tilde{T}$ is the m x n transfer matrix. If the F's and M's are not linearly related, as would be the case if dipole location was a parameter in the model, we can linearize the equations about a point in model space. Non-linear examples will be treated in a later section.

In particular, each element T_{ij} represents the value of the i^{th} field measurement, i.e. F_i, if only one model term M_j contributes, i.e. $M_k = \delta_{kj}$. Thus a horizontal row of $\tilde{T}$ corresponds to the field equation for the complete model and describes how a particular measurement is affected by each source term, while each column of $\tilde{T}$ describes how a particular source term affects each of the measurements. If there are more measurements than model parameters, Eq. (2.1) will represent an overdetermined set of equations. However, it is possible that a pair of model parameters may not be totally independent, resulting in coupled columns in $\tilde{T}$. Then $\tilde{T}$ might be singular so that the set of equations will not have a unique solution for $\tilde{M}$ given $\tilde{T}$ and $\tilde{F}$. Similarly, if two or more field measurements are linearly related, two or more rows of $\tilde{T}$ would be linearly dependent. This will pose a problem if there is an insufficient number of independent field measurements to solve Eq. (2.1) for the model parameters.

As a simple, two dimensional example of how a set of data relates to a model, let the model be a magnetic dipole $\vec{m}$ located at a known point $\vec{r}'$. We will attempt to make measurements of B_x at points $\vec{r}_1$ and $\vec{r}_2$ in order to determine the unknown dipole components m_x and m_y. The magnetic induction $\vec{B}$ is given by

$$\vec{B}(r) = \frac{\mu_o}{4\pi} \; \frac{3\vec{m}\cdot(\vec{r}-\vec{r}')}{|\vec{r}-\vec{r}'|} \, (\vec{r}-\vec{r}') - \frac{\vec{m}}{|\vec{r}-\vec{r}|^3} \qquad (2.3)$$

so that B_x satisfies the equation

$$B_x(r) = \frac{\mu_o}{4\pi}\left\{ \frac{\left[3\, m_x(x-x') + m_y(y-y')\right]}{|\vec{r}-\vec{r}'|^5}(x-x') - \frac{m_x}{|\vec{r}-\vec{r}'|^3} \right\} \qquad (2.4)$$

For two B_x measurements, we will have two simultaneous equations, linear in $\vec{m}$, that are of the form of Eq. (2.4). We must determine the values of $\vec{r}_1$ and $\vec{r}_2$ for which these two equations have a unique solution. As we will see, sensitivity vectors will allow us to do this and also to identify the optimum values of $\vec{r}_1$ and $\vec{r}_2$.

We can define vector spaces for both the field measurements and the model parameters, so that the elements of $\tilde{F}$ and $\tilde{M}$ become the components of vectors $\vec{F}$ and $\vec{M}$. As an aid in understanding the relationship of several measurements to the model, we can define a gradient operator in model space by

$$\vec{\nabla}_M = \frac{\partial}{\partial M_1}\hat{i} + \frac{\partial}{\partial M_2}\hat{j} + \frac{\partial}{\partial M_3}\hat{k} + . . . \frac{\partial}{\partial M_m}\hat{m} \qquad (2.5)$$

where $\hat{i}$, $\hat{j}$, $\hat{k}$, $\hat{m}$ are the unit vectors in each direction in model space. In our two-dimensional example,

$$\vec{\nabla}_M = \frac{\partial}{\partial m_x}\hat{i} + \frac{\partial}{\partial m_y}\hat{j} \qquad (2.6)$$

The sensitivity vector for measurement F_i is defined by

$$\vec{S}_i = \nabla_M \vec{F}_i \qquad (2.7)$$

The interpretation of $\vec{S}_i$ is straightforward: $\vec{S}_i$ indicates the direction of the change in model $\tilde{M}$ that produces the maximum change in the measurement F_i. Any change in $\tilde{M}$ that is perpendicular to $\vec{S}_i$ will be undetected by F_i. Thus, the direction of the sensitivity vector can be used to determine the source configuration for which F_i has the maximum sensitivity and the configuration which is not detected by F_i. The magnitude of the sensitivity vector is proportional to the maximum field produced at the measurement point by a given strength source and can be used to determine the relative sensitivities of several measurements.

For linear systems, the components of the sensitivity vector for a particular measurement F_i is in fact a row of $\tilde{T}$. To show this, we can write Eq. (2.2) as

$$F_i = \sum_j T_{ij} M_j \tag{2.8}$$

and Eq. (2.7) as

$$\vec{S}_i = \sum_{k=1}^{m} \frac{\partial}{\partial M_k} (F_i)\,\hat{e}_k = \sum_{k=1}^{m} \frac{\partial}{\partial M_k} \left(\sum_{j=1}^{n} T_{ij} \; M_j \right) \hat{e}_k \tag{2.9}$$

where $\hat{e}_k$ is the k^{th} unit vector.

Since the T_{ij} are independent of M, this becomes

$$\vec{S}_i = \sum_{j,k=1}^{m} T_{ij} \frac{\partial}{\partial M_k} (M_j)\,\hat{e}_k$$

(2.10)

$$\sum_{j>k=1}^{m} T_{ij} \; \delta_{jk} \hat{e}_k = \sum_{k=1}^{m} T_{ik} \hat{e}_k$$

Thus $\vec{S}_i$ is a vector in model space whose components are the i^{th} row of $\tilde{T}$. While we have obtained this simple result from an apparently circuitous route, it provides us with a better understanding of the significance of each row: S_i and the i^{th} of $\tilde{T}$ can be used to determine the sensitivity of F_i to changes in the model $\vec{M}$, and $\vec{S}_i$ vectors can be plotted to help visualize how measurement sensitivity depends upon measurement location. For non-linear systems, which can not be described using equations of the form of Eq. (2.1) and (2.2), we will show subsequently that the sensitivity vectors are still valid and can be readily determined analytically or numerically without explicitly linearizing the system of equations.

particular measurement F_i is in fact a row of $\tilde{T}$. To show this, we can write Eq. (2.2) as

$$F_i = \sum_j T_{ij} M_j \tag{2.8}$$

and Eq. (2.7) as

$$\vec{S}_i = \sum_{k=1}^{m} \frac{\partial}{\partial M_k} (F_i)\, \hat{e}_k = \sum_{k=1}^{m} \frac{\partial}{\partial M_k} \left(\sum_{j=1}^{n} T_{ij}\, M_j \right) \hat{e}_k \tag{2.9}$$

where $\hat{e}_k$ is the k^{th} unit vector.

Since the T_{ij} are independent of M, this becomes

$$\vec{S}_i = \sum_{j,k=1}^{m} T_{ij} \frac{\partial}{\partial M_k} (M_j)\, \hat{e}_k$$

$$= \sum_{j>k=1}^{m} T_{ij}\, \delta_{jk} \hat{e}_k = \sum_{k=1}^{m} T_{ik}\, \hat{e}_k \tag{2.10}$$

Thus $\vec{S}_i$ is a vector in model space whose components are the i^{th} row of $\tilde{T}$. While we have obtained this simple result from an apparently circuitous route, it provides us with a better understanding of the significance of each row: S_i and the i^{th} of $\tilde{T}$ can be used to determine the sensitivity of F_i to changes in the model $\vec{M}$, and $\vec{S}_i$ vectors can be plotted to help visualize how measurement sensitivity depends upon measurement location. For non-linear systems, which can not be described using equations of the form of Eq. (2.1) and (2.2), we will show subsequently that the sensitivity vectors are still valid and can be readily determined analytically or numerically without explicitly linearizing the system of equations.

III. A TWO-DIMENSIONAL DIPOLE MODEL

In the simple two-dimensional model of a magnetic dipole $\vec{m}$ with components m_x and m_y, the field in the x-direction is given by Eq. (2.4). The sensitivity vector becomes

$$\vec{S}(\vec{r}, \vec{r}') = \vec{\nabla}_m B_x(\vec{r}) \tag{3.1}$$

or, after dropping the $\frac{\mu_o}{4\pi}$ for convenience,

$$\vec{S}(\vec{r}, \vec{r}') = \frac{1}{|\vec{r} - \vec{r}'|^5} \left\{ \left[3(x - x')^2 - |\vec{r} - \vec{r}'|^2\right]\hat{i} + 3(x - x')(y - y')\hat{j} \right\} \tag{3.2}$$

If the dipole is at the origin, r' = 0 and

$$\vec{S}(\vec{r}, \vec{r}) = \frac{1}{r^5} \left\{ (3x^2 - r^2)\hat{i} + 3xy\hat{j} \right\} \tag{3.3}$$

We can use Eq. (3.3) to calculate the sensitivity vectors for measurements of B_x in the xy plane. It follows that

$$S_x = \frac{1}{r^5}(3x^2 - r^2) \qquad S_y = \frac{3xy}{r^5} \tag{3.4}$$

If all measurements are made at the same distance from origin then $|\vec{r}| = \sqrt{x^2 + y^2} = 1$ and

$$S_x = 3x^2 - 1 \qquad S_y = 3xy \tag{3.5}$$

The sensitivity vector components and magnitudes at sixteen points are listed in Table 3.1 and plotted in Figure 3.1. Several important features are immediately obvious. At points A and E, a measurement of B_x detects

TABLE 3.1

Sensitivity vectors at several points equidistant from a dipole. The data are plotted in Fig. 3.1.

POINT	X Y	S_x	S_y	$\|\vec{S}\|$
A	± 1.00 0.00	2.00	0.00	2.00
B	± 0.87 0.49	1.281	± 1.281	1.81
C	± 0.58 0.82	0.00	± 1.41	1.41
D	± 0.27 0.96	-0.78	± 0.78	1.10
E	0.00 ± 1.00	-1.00	0.00	1.00

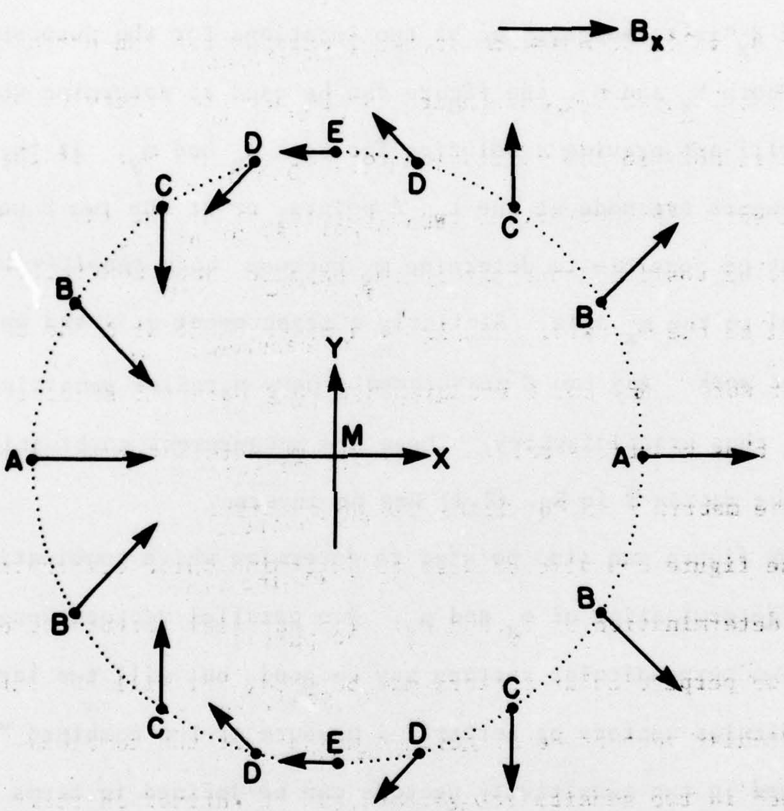

Figure 3.1. The sensitivity vectors for measurements of B_x at unit distance from a fixed magnetic dipole. The coordinates of the points are listed in Table 3.1.

fields from m_x but not from m_y. The sensitivity at A is twice that at E. At point C, m_y is detected but not m_x. The sensitivity components S_x and S_y are equal to each other at point B and at point D, but the magnitude of $\vec{S}$ is 1.81 at B and only 1.10 at D.

If B_x is to be measured at two locations for the purpose of determining both m_x and m_y, the figure can be used to determine which combinations will not provide a solution for both m_x and m_y. If the two B_x measurements are made at the two A points, or at the two E points, it will not be possible to determine m_y because both sensitivity vectors are parallel to the m_x axis. Similarly a measurement at A and another at E will not work Any two C measurements have parallel sensitivity vectors and are thus unsatisfactory. These are measurement combinations for which the matrix $\tilde{T}$ in Eq. (2.2) has no inverse.

The figure can also be used to determine which combinations provide a good determination of m_x and m_y. Two parallel vectors were shown to be bad. Two perpendicular vectors may be good, but will two larger, non-perpendicular vectors be better? A measure of the combined "information" contained in two sensitivity vectors can be defined in terms of the magnitude of their cross-product

$$V = |\vec{S}_1 \times \vec{S}_2| \tag{3.6}$$

If $\vec{S}_1$ and $\vec{S}_2$ are parallel, $V = 0$. If $\vec{S}_1$ and $\vec{S}_2$ are perpendicular, V will be large. In the two-dimensional example

$$V = |S_{x_1} S_{y_2} - S_{y_1} S_{x_2}| \tag{3.7}$$

For two B measurements in adjacent quadrants, V = 3.28, for two D measurements, V = 1.22, implying that in the presence of noise, it would be significantly better to measure B_x at adjacent B points than at adjacent D points. The values of V for pairs of measurement points in the first and second quadrants are listed in Table 3.2. As might be expected from the figure, adjacent D and E points have a low V value of 0.78. Note the symmetry of the table across the heavy-lined boxes.

As a second example, suppose we have a single vector magnetometer that measures B_x and B_y at a single point (x, y). If the model is a dipole located at the origin and lying in the x-y plane, the sensitivity vector for each field component is given by

$$\vec{S}(B_x) = \frac{1}{r^5}\left[(3x^2 - r^2)\hat{i} + (3xy)\hat{j}\right]$$
$$\vec{S}(B_y) = \frac{1}{r^5}\left[(3xy)\hat{i} + (3y^2 - r^2)\hat{j}\right] \tag{3.8}$$

The cross product V becomes

$$V = |S_x(B_x)S_y(B_y) - S_y(B_x)S_x(B_y)|$$

$$= \frac{1}{r^{10}}\left|(3x^2 - r^2)(3y^2 - r^2) - (3xy)(3xy)\right| = \frac{2}{r^6} \tag{3.9}$$

This result indicates that the ability of a vector magnetometer to determine the components of the dipole depends solely on the distance of the magnetometer from the dipole, and not upon the relative orientation of the dipole and the magnetometer. This is apparent in Fig. 3.2, which

TABLE 3.2

The quantity $V = |S_{x_1} S_{y_2} - S_{y_1} S_{x_2}|$ computed for pairs of B_x measurement points in the first and second quadrants for the sensitivity vectors in Table 3.1.

	FIRST QUADRANT					SECOND QUADRANT			
	A	B	C	D	E	D	C	B	A
A	$\boxed{0}$	2.56	2.82	1.56	0	1.56	2.82	2.56	$\boxed{0}$
B	2.56	$\boxed{0}$	1.80	2.00	1.28	0	1.80	$\boxed{3.28}$	2.56
C	2.82	1.80	$\boxed{0}$	1.10	1.41	1.10	$\boxed{0}$	1.80	2.82
D	1.56	2.00	1.10	$\boxed{0}$	0.78	$\boxed{1.22}$	1.10	0	1.56
E	0	1.28	1.41	0.78	$\boxed{0}$	0.78	1.41	1.28	0

(Rows: FIRST QUADRANT)

TABLE 3.3

The coordinates and sensitivity vector components for B_x and B_y measurements in the first quadrant. The data are plotted in Fig. 3.2.

Location	Coordinates	B_x: S_x	B_x: S_y	B_y: S_x	B_y: S_y
A	1.00, 0.00	2.000	0	0	-1.000
B	0.92, 0.38	1.561	1.062	1.062	-0.560
C	0.71, 0.71	0.500	1.500	1.500	0.500
D	0.38, 0.92	-0.560	1.062	1.062	1.561
E	0.00, 1.00	-1.000	0	0	2.000

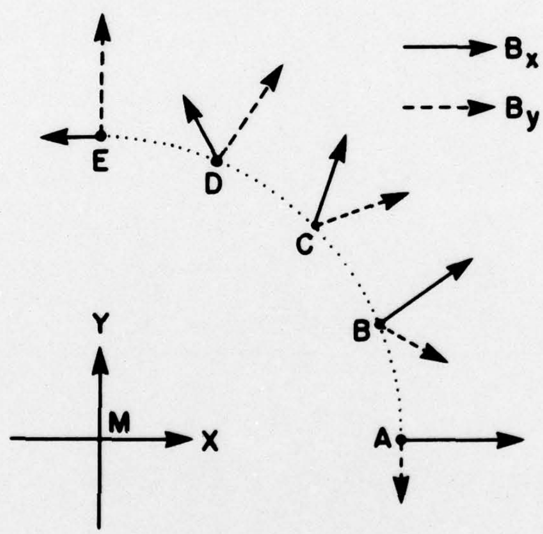

Figure 3.2. The sensitivity vectors for measurements of B_x and B_y at unit distance from a fixed magnetic dipole. The coordinates of the points are listed in Table 3.2.

shows the B_x and B_y sensitivity vectors for a vector magnetometer at a constant distance from the dipole. At locations A and E, the B_x magnetometer is sensitive only to m_x, while the B_y magnetometer is sensitive only to m_y. Thus the calculation of $\vec{m}$ from $\vec{B}$ can be performed with equal accuracy at all points on the circle in the figure. We will show later that the location of a vector magnetometer becomes significant when using a model with higher-order moments.

IV. THE INFORMATION MATRIX

While the quantity V provides a measure of sensitivity and the ability to invert the transfer matrix to determine the model parameters, we need more complex models and thus must find a multidimensional equivalent of V. Extension of Eq. 3.5 to three dimensions is straightforward, with V defined by the vector triple product

$$V = \vec{S}_1 \cdot (\vec{S}_2 \times \vec{S}_3) = \vec{S}_2 \cdot (\vec{S}_3 \times \vec{S}_1) = \vec{S}_3 \cdot (\vec{S}_1 \times \vec{S}_2) \qquad (4.1)$$

Note that V is equal to the volume in model space enclosed by the three sensitivity vectors. If any two of the vectors are parallel, $V = 0$. We see that for a three parameter model, V measures how well the sensitivity vectors for a set of measurements "span" model space. In the absence of noise or computational inaccuracy, an n parameter model can ideally be specified using n measurements that have orthogonal sensitivity vectors spanning model space. In the three-dimensional case, three measurements are required but additional measurements may increase V either because some of the measurements may have low sensitivity or non-orthogonal sensitivity vectors.

In order to extend V to more than three dimensions, we need to introduce the information matrix. The j^{th} component of the sensitivity vector for the i^{th} measurement is $(\vec{S}_i)_j$ and is given by Eq. (2.10)

$$(\vec{S}_i)_j = T_{ij} \qquad (4.2)$$

so we can rewrite Eq. (2.8) as

$$F_i = \sum_j T_{ij} M_j = \sum_j (\vec{S}_i)_j M_j = \tilde{S}_i^T \tilde{M} \qquad (4.3)$$

where $\tilde{S}_i^T$ is the transpose of the column matrix equivalent to $\vec{S}_i$. We can multiply Eq. (4.3) on the left by $\tilde{S}_i$ to obtain, for an m dimensional model,

$$\tilde{S}_i F_i = \tilde{S}_i \tilde{S}_i^T \tilde{M} = \tilde{R}_i \tilde{M} \tag{4.4}$$

where $\tilde{R}_i$ is termed the "information matrix" and is an m x m square, symmetric matrix particular to the i^{th} measurement. If there are n measurements, the n equations of this form can be summed to yield

$$\sum_{i=1}^{n} \tilde{S}_i F_i = \sum_{i=1}^{n} (\tilde{S}_i \tilde{S}_i^T)\tilde{M} = \left[\sum_{i=1}^{n} \tilde{R}_i\right] \tilde{M} \tag{4.5}$$

which can be solved for $\tilde{M}$

$$\tilde{M} = \left[\sum_{i=1}^{n} \tilde{R}_i\right]^{-1} \sum_{i=1}^{n} \tilde{S}_i F_i = \tilde{R}^{-1} \sum_{i=1}^{n} \tilde{S}_i F_i \tag{4.6}$$

with $\tilde{R}$ being the m x m information matrix for the entire set of measurements. Equation (4.6) represents a solution to the "inverse problem" in which field data are used to determine certain source parameters. In the equation, the n F_i will be known, since these are the field measurements, and the $\tilde{S}_i$ and $\tilde{R}$ can be calculated for the chosen model. However, if $\tilde{R}$ does not have an inverse, we cannot determine $\tilde{M}$.

As an example of this, let us return to the two-dimensional dipole example in Section 3. If measurements are made at points A and E, the sensitivity vectors and information matrices will be

$$\tilde{S}_1 = \begin{pmatrix} 2.0 \\ 0.0 \end{pmatrix}$$

$$\tilde{R}_1 = S_1 S_1^T = \begin{pmatrix} 2.0 \\ 0.0 \end{pmatrix} (2.0 \quad 0.0) = \begin{pmatrix} 4.0 & 0.0 \\ 0.0 & 0.0 \end{pmatrix}$$

$$\tilde{S}_2 = \begin{pmatrix} -1.0 \\ 0.0 \end{pmatrix} \quad \tilde{R}_2 = \begin{pmatrix} 1.0 & 0.0 \\ 0.0 & 0.0 \end{pmatrix} \tag{4.7}$$

$$\tilde{R} = \tilde{R}_1 + \tilde{R}_2 = \begin{pmatrix} 5.0 & 0.0 \\ 0.0 & 0.0 \end{pmatrix}$$

Because $\tilde{R}$ has a zero determinant, it has no inverse and we can not determine both dipole components. This is as expected, since for these two measurements, V = 0.

We can make the connection between the determinant of $\tilde{R}$ and V by writing

$$\tilde{S}_1 = \begin{pmatrix} S_{11} \\ S_{12} \end{pmatrix} \qquad \tilde{S}_2 = \begin{pmatrix} S_{21} \\ S_{22} \end{pmatrix} \tag{4.8}$$

and computing $\det|\tilde{R}|$

$$\det|\tilde{R}| = (S_{21}S_{12} - S_{11}S_{22})^2 = V^2 \tag{4.9}$$

to find that our n-dimensional V is simply

$$V = (\det|\tilde{R}|)^{1/2} \tag{4.10}$$

We now see that V, which provides a measure of how well a set of measurements span the model space, is also a measure of how readily the information matrix can be inverted as required to solve the inverse problem. Given this introduction to $\tilde{S}_i$, V, and $\tilde{R}$, we are now prepared to work several examples.

4.1. The Two-Dimensional Dipole

Equation 4.4 and the data listed in Table 3.1 can be used to compute the information matrix for each measurement in quadrants I and II in Fig. 3.1, and the information matrix for all pairs of measurements. The results, listed in Table 4.1, are consistent with Table 3.2 and show that certain pairs such as A1-A2, A1-E1 and C1-C2 have a singular information matrix. The pair B1-B2 had the largest value V in Table 3.2 and is now seen to have a diagonal information matrix with large, equal eigenvalues. In this case, $\tilde{R}$ can be written as

$$\tilde{R} = \lambda \tilde{I} \tag{4.11}$$

where λ is the eigenvalue and $\tilde{I}$ is the identity matrix. Equation 4.6 reduces to

$$\tilde{M} = \lambda^{-1} \sum_{i=1}^{n} \tilde{S}_i F_i \tag{4.12}$$

The j^{th} component of $\tilde{M}$ becomes

$$M_j = \lambda^{-1} \sum_{i=1}^{n} (S_i)_j F_i = \lambda^{-1} \sum_{i=1}^{n} T_{ij} F_i \tag{4.13}$$

We recognize the summation as a matrix multiplication and write

$$\tilde{M} = \lambda^{-1} \tilde{T}^T \tilde{F} \tag{4.14}$$

Thus for properly chosen measurement points, solution of the inverse problem reduces to a trivial matrix multiplication using the transpose of the original $\tilde{T}$ matrix. This is the motivation for finding sets of

	FIRST QUADRANT										SECOND QUADRANT							
	A		B		C		D		E		D		C		B		A	
	4.00	0	1.64	1.64	0	0	0.61	-0.61	1.00	0	0.61	0.61	0	0	1.64	-1.64	4.00	0
	0	0	1.64	1.64	0	1.99	-0.61	0.61	0	0	0.61	0.61	0	1.99	-1.64	1.64	0	0
FIRST QUADRANT A	8.00	0	5.64	1.64	4.00	0	4.61	-0.61	5.00	0	4.61	0.61	4.00	0	5.64	-1.64	8.00	0
	0	0	1.64	1.64	0	1.99	-0.61	0.61	0	0	0.61	0.61	0	1.99	-1.64	1.64	0	0
B			3.28	3.28	1.64	1.64	2.25	1.03	2.64	1.64	2.25	2.25	1.64	1.64	3.28	0		
			3.28	3.28	1.64	3.63	1.03	2.25	1.64	1.64	2.25	2.25	1.64	3.63	0	3.28		
C					0	0	0.61	-0.61	1.00	0	0.61	0.61	0	0				
					0	3.98	-0.61	2.60	0	1.99	0.61	2.60	0	3.98				
D							1.22	-1.22	1.61	-0.61	1.22	0						
							-1.22	1.22	-0.61	0.61	0	1.22						
E									2.00	0								
									0	0								

Table 4.1. The information matrices for each of the measurement points and pairs of points in Table 3.2.

measurement points where the sensitivity vectors are orthonormal.

As an example of this, let us assume that we can make one B_x field measurement at the arbitrary point (0.75, 0.66), between points B and C in Fig. 3.1, and that we want to find the second point so that $\tilde{R}$ is diagonal and has equal eigenvalues. Using Eq. (3.3), we find that $\tilde{S}_1$ and $\tilde{S}_2$ will be

$$\tilde{S}_1 = \begin{pmatrix} 0.69 \\ 1.49 \end{pmatrix}$$

$$\tilde{S}_2 = \frac{1}{r^5} \begin{pmatrix} 2x^2 - y^2 \\ 3xy \end{pmatrix} = \begin{pmatrix} A \\ B \end{pmatrix} \tag{4.15}$$

The information matrix for these two measurements is

$$\tilde{R} = \frac{1}{r^{10}} \begin{pmatrix} (2x^2 - y^2)^2 + 0.48r^{10} & 3xy(2x^2 - y^2) + 1.03r^{10} \\ 3xy(2x^2 - y^2) + 1.03r^{10} & (3xy)^2 + 2.22r^{10} \end{pmatrix} \tag{4.16}$$

Rather than use Eq. (4.16) to find the values of x and y where $\tilde{R}$ is diagonal and has equal eigenvalues, it is more convenient to determine the points where

$$|\vec{S}_1| = |\vec{S}_2| \quad \text{and} \quad \vec{S}_1 \cdot \vec{S}_2 = 0 \tag{4.16}$$

From Eqs. (4.15), it follows that Eq. (4.16) is satisfied by

$$\vec{S}_2 = \pm 1.49\ \hat{x} \mp 0.69\ \hat{y} \tag{4.17}$$

Visual examination of Fig. 3.1 shows that the points with this sensitivity will be located approximately as follows

$$\begin{array}{l} \text{Quadrants I \& III between D \& E,} \quad r < 1 \\ \text{Quadrants II \& IV between A \& B,} \quad r > 1 \end{array} \tag{4.18}$$

We can now proceed to calculate the locations exactly using Eqs. (4.15) and (4.17)

$$\frac{1}{r^5}(2x^2 - y^2) = \pm 1.49$$
$$\frac{1}{r^5}(3xy) = \mp 0.69 \qquad (4.19)$$

The most direct method of solving these simultaneous, non-linear equations is to solve first for r and then for x and y, which gives the values

$$\begin{array}{ll} r = 1.057 & r = 0.856 \\ x = \pm 1.013 & x = \pm 0.125 \\ y = \mp 0.299 & y = \pm 0.847 \end{array} \qquad (4.20)$$

These data are plotted in Fig. 4.1. The significance of this calculation is that the results were predicted approximately using Fig. 3.1. Thus one strength of sensitivity vectors is their suitability visualizing measurement sensitivity.

4.2 The Single Vector Magnetometer

We can now use the information matrix to examine the vector magnetometer example discussed in Section 3. If the magnetometer measures B_x and B_y at a point (x, y), Eqs. (3.8) can be used to compute the information matrices for measurements of B_x and B_y:

$$\tilde{R}_i = \tilde{S}_i \tilde{S}_i^T$$

$$\tilde{R}_{B_x} = \frac{1}{r^{10}} \begin{pmatrix} (3x^2 - r^2)^2 & 3xy(3x^2 - r^2) \\ 3xy(3x^2 - r^2) & (3xy)^2 \end{pmatrix} \qquad (4.21)$$

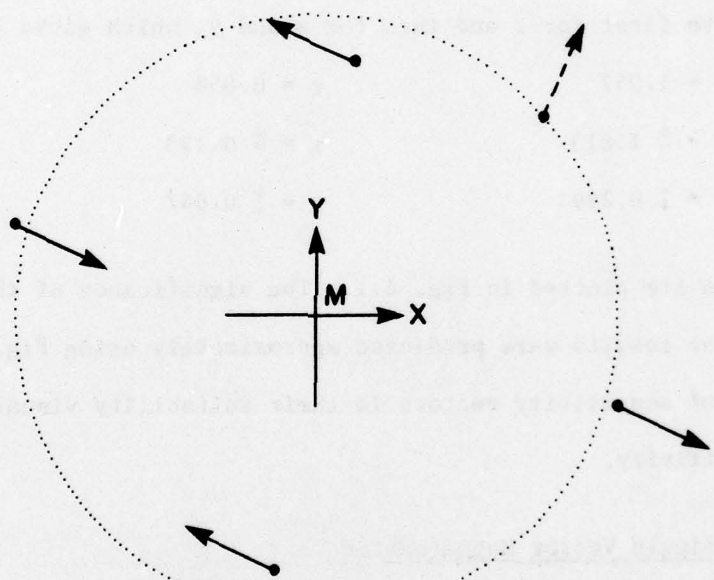

Fig. 4.1. Four locations where the B_x sensitivity vector (solid) is perpendicular to the dashed vector and has the same magnitude.

$$\tilde{R}_{B_y} = \frac{1}{r^{10}} \begin{pmatrix} (3xy)^2 & 3xy(3y^2 - r^2) \\ 3xy(3y^2 - r^2) & (3y^2 - r^2)^2 \end{pmatrix} \qquad (4.21 \text{ cont'd})$$

The information matrix for a vector magnetometer is given by

$$\tilde{R}_V = \tilde{R}_{B_x} + \tilde{R}_{B_y}$$

$$= \frac{1}{r^8} \begin{pmatrix} 4x^2 + y^2 & 3xy \\ 3xy & x^2 + 4y^2 \end{pmatrix} \qquad (4.22)$$

It follows immediately that

$$\det |\tilde{R}| = \frac{4}{r^{12}}$$

and, consistent with the previous result in section III,

$$V = \left[\det |\tilde{R}|\right]^{1/2} = \frac{2}{r^6} \qquad (4.23)$$

Since V is determined by r but is independent of x and y, this shows that there is no optimum position for the vector magnetometer for a fixed distance from the dipole. Equation (4.22) also shows that $\tilde{R}$ is diagonal for measurements on either the x or y axes.

In a later section, we will extend this example to include different noise in the x and y axis magnetometers.

4.3 Multiple B_x and B_y Magnetometers

The analysis techniques developed in the preceeding sections can be applied to the row of either 11 B_x or 11 B_y single-axis magnetometers shown in Fig. 4.2. The sensitivity vectors and information matrices for each magnetometer are listed in Tables 4.2 and 4.3, with the source assumed to be

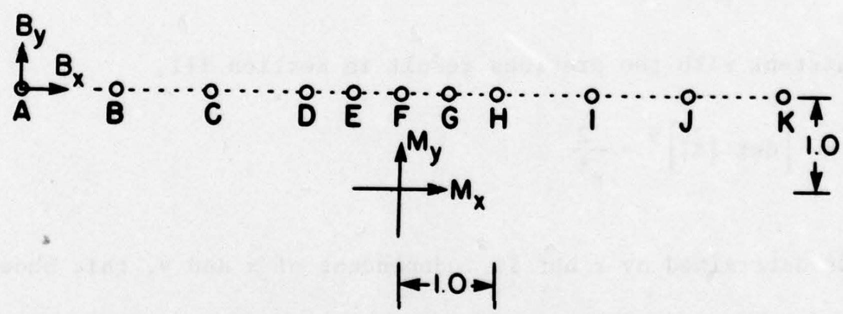

Fig. 4.2. A row of B_x or B_y magnetometers near a magnetic dipole.

TABLE 4.2

Sensitivity vectors and information matrices for the line of B_x magnetometers in Figure 4.2. $S_x = (3x^2 - r^2)r^{-5}$, $S_y = 3xy\ r^{-5}$

Position	Coordinates	r	S_x	S_y	$\lvert\vec{S}\rvert$	$\tilde{R}$
A	-4.0, 1.0	4.12	0.026	-0.010	0.028	$\begin{pmatrix} 0.001 & 0.000 \\ 0.000 & 0.000 \end{pmatrix}$
B	-3.0, 1.0	3.16	0.054	-0.028	0.061	$\begin{pmatrix} 0.003 & -0.002 \\ -0.002 & 0.001 \end{pmatrix}$
C	-2.0, 1.0	2.24	0.125	-0.107	0.165	$\begin{pmatrix} 0.016 & -0.013 \\ -0.013 & 0.011 \end{pmatrix}$
D	-1.0, 1.0	1.41	0.177	-0.530	0.559	$\begin{pmatrix} 0.031 & -0.094 \\ -0.094 & 0.281 \end{pmatrix}$
E	-0.5, 1	1.12	-0.286	-0.859	0.905	$\begin{pmatrix} 0.082 & 0.246 \\ 0.246 & 0.738 \end{pmatrix}$
F	0.0, 1.0	1.0	-1.000	0	1.000	$\begin{pmatrix} 1.000 & 0.000 \\ 0.000 & 0.000 \end{pmatrix}$
G	0.5, 1.0	1.12	-0.286	0.859	0.905	$\begin{pmatrix} 0.082 & -0.246 \\ -0.246 & 0.738 \end{pmatrix}$
H	1.0, 1.0	1.41	0.177	0.530	0.559	$\begin{pmatrix} 0.031 & 0.094 \\ 0.094 & 0.281 \end{pmatrix}$
I	2.0, 1.0	2.24	0.125	0.107	0.165	$\begin{pmatrix} 0.016 & 0.013 \\ 0.013 & 0.011 \end{pmatrix}$
J	3.0, 1.0	3.16	0.054	0.028	0.061	$\begin{pmatrix} 0.003 & 0.002 \\ 0.002 & 0.001 \end{pmatrix}$
K	4.0, 1.0	4.12	0.026	0.010	0.028	$\begin{pmatrix} 0.001 & 0.000 \\ 0.000 & 0.000 \end{pmatrix}$

TABLE 4.3

Sensitivity vectors and information matrices for the line of B_y magnetomers in Figure 4.2. $S_x = 3xy\ r^{-5}$, $S_y = (3y^2 - r^2)r^{-5}$.

Position	Coordinates	r	S_x	S_y	$\lvert S \rvert$	$\tilde{R}$
A	-4.0, 1.0	4.12	-0.010	-0.012	0.015	$\begin{pmatrix} 0.000 & 0.000 \\ 0.000 & 0.000 \end{pmatrix}$
B	-3.0, 1.0	3.16	-0.028	-0.022	0.036	$\begin{pmatrix} 0.001 & 0.001 \\ 0.001 & 0.000 \end{pmatrix}$
C	-2.0, 1.0	2.24	-0.107	-0.036	0.113	$\begin{pmatrix} 0.011 & 0.004 \\ 0.004 & 0.001 \end{pmatrix}$
D	-1.0, 1.0	1.41	-0.530	0.177	0.559	$\begin{pmatrix} 0.281 & -0.094 \\ -0.094 & 0.031 \end{pmatrix}$
E	-0.5, 1.0	1.12	-0.859	1.002	1.319	$\begin{pmatrix} 0.738 & -0.861 \\ -0.861 & 1.004 \end{pmatrix}$
F	0.0, 1.0	1.0	0	2.000	2.000	$\begin{pmatrix} 0.000 & 0.000 \\ 0.000 & 4.000 \end{pmatrix}$
G	0.5, 1.0	1.12	0.859	1.002	1.319	$\begin{pmatrix} 0.738 & 0.861 \\ 0.861 & 1.004 \end{pmatrix}$
H	1.0, 1.0	1.41	0.530	0.177	0.559	$\begin{pmatrix} 0.281 & 0.094 \\ 0.094 & 0.031 \end{pmatrix}$
I	2.0, 1.0	2.24	0.107	-0.036	0.113	$\begin{pmatrix} 0.011 & -0.004 \\ -0.004 & 0.001 \end{pmatrix}$
J	3.0, 1.0	3.16	0.028	-0.022	0.036	$\begin{pmatrix} 0.001 & -0.001 \\ -0.001 & 0.000 \end{pmatrix}$
K	4.0, 1.0	4.12	0.010	-0.012	0.015	$\begin{pmatrix} 0.000 & 0.000 \\ 0.000 & 0.000 \end{pmatrix}$

a dipole located at the origin. The sensitivity vectors are plotted in Figs. 4.3 and 4.4 both as scalar functions of x and as vectors at each measurement point.

The plots of S_x and S_y versus x in Fig. 4.3 can be seen to correspond to plots of the B_x field of the m_x and m_y dipole components, respectively. This will be explained in terms of the reciprocity theorem in Section 6. Examination of the S_x and S_y curves can be used to choose optimum locations for a B_x magnetometer. For example B_x measured at E and G would be good for determining m_y, but B_x at F would be more sensitive to m_x. Choice of measurement locations is simplified by the vector plot in the lower half of the figure. The three largest vectors are at E, F, and G and appear to span the dipole space relatively well. Addition of points D and H will make only small improvements, since these vectors are significantly smaller than the parallel vectors at G and E, respectively.

The plots in Fig. 4.4 show that the sensitivity of B_y to m_x is the same as that of B_x to m_y, but B_y is twice as sensitive to m_y as B_x is to m_x. Thus, for a row of magnetometers displaced from the source in y direction, measurements of B_y are superior to measurements of B_x. The vector plot in Fig. 4.4 shows that B_y measurements at locations E and G have large, nearly perpendicular sensitivity vectors. Both figures show that there is a serious loss in sensitivity for measurement locations for which $x > 2y$.

Given the sensitivity vector data and information matrices listed in Tables 4.2 and 4.3, we can calculate the quantity V for various combinations of B_x and B_y measurements, as listed in Table 4.4. Several important points become apparent in the table. A vector magnetometer at (0.0, 1.0) has a V of 2.0, greater than any of the combinations of 2 to 11

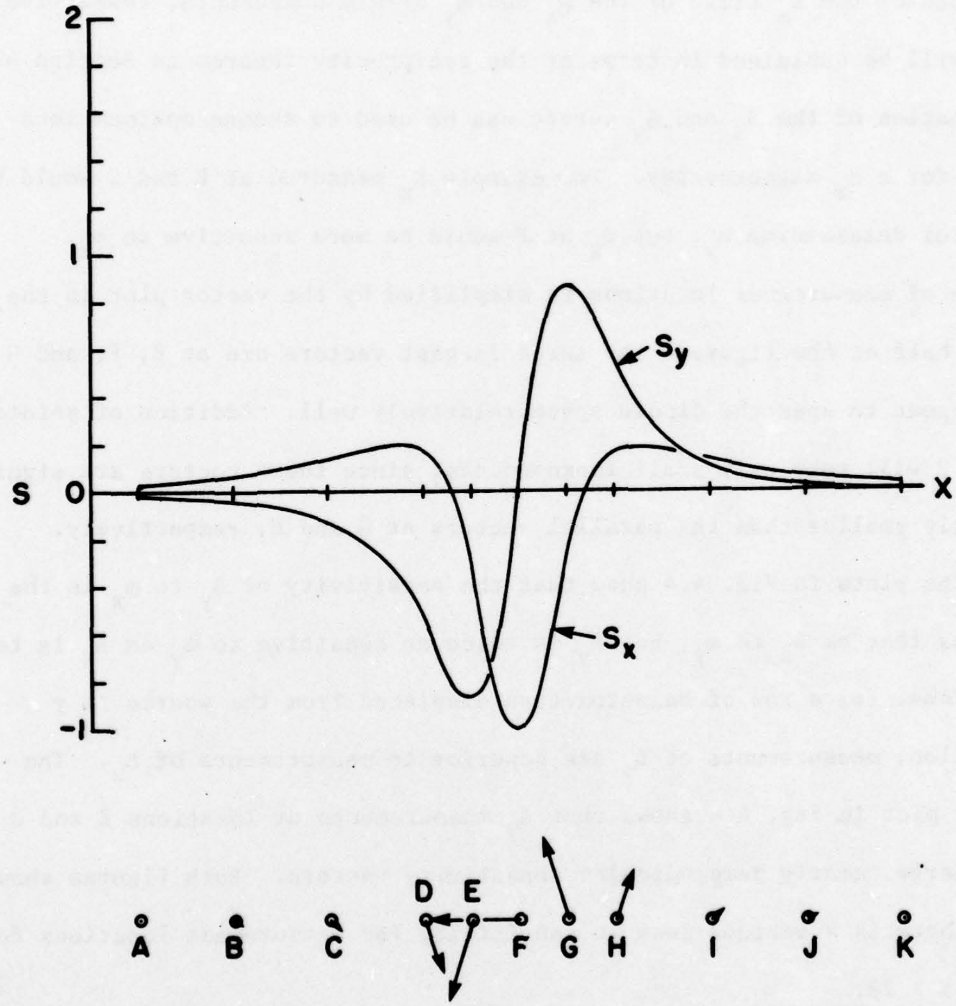

Fig. 4.3 (Upper). The quantities S_x and S_y plotted as a function of x for the B_x magnetometers in Fig. 4.2. (Lower). A vector plot of $\vec{S}$ for the same data.

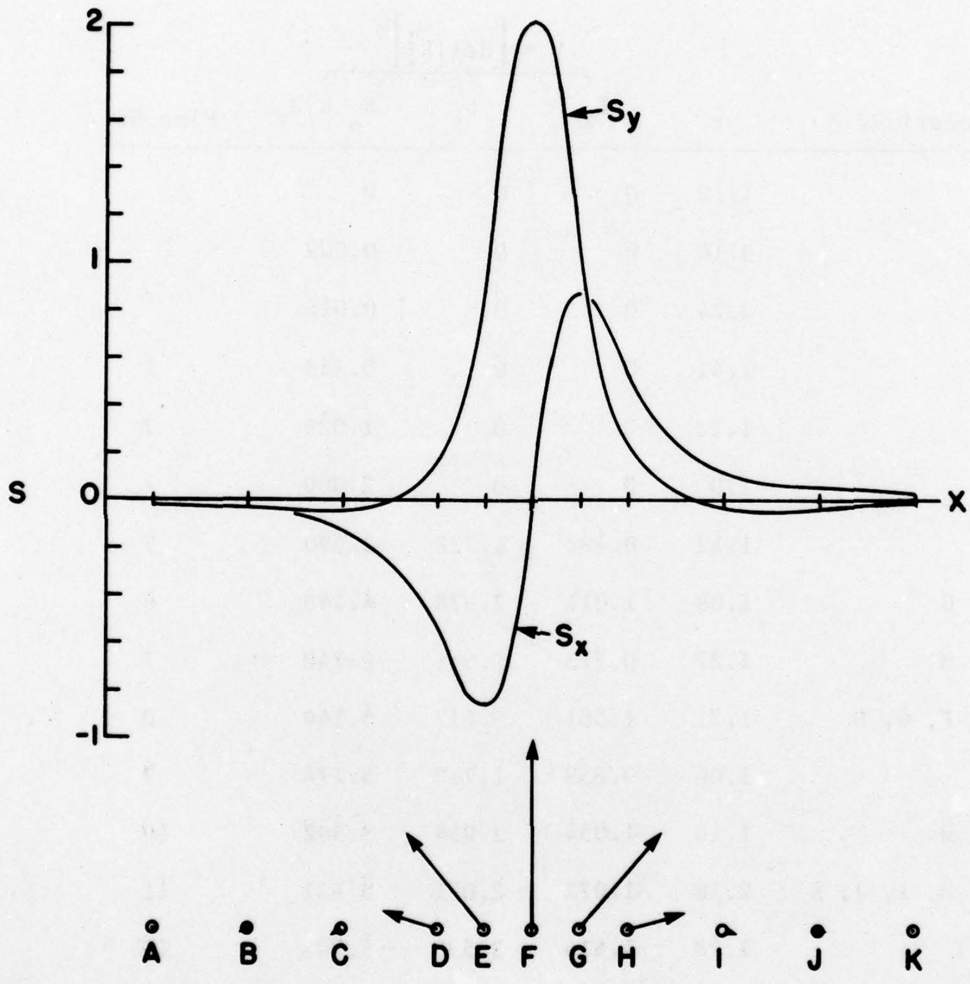

Fig. 4.4 (Upper). The quantities S_x and S_y plotted as a function of x for the B_y magnetometers in Fig. 4.2. (Lower). A vector plot of $\vec{S}$ for the same data.

TABLE 4.4

The quantity V for various combinations of B_x and B_y magnetometers. The locations are shown in Fig. 4.2. The mean distance of the measurements to the dipole is listed under $\bar{r}$.

		$V = \left[\det\lvert\tilde{R}\rvert\right]^{1/2}$			
Locations	$\bar{r}$	B_x	B_y	B_x & B_y	Plot No.
A	4.12	0	0	0	
B	3.16	0	0	0.002	
C	2.24	0	0	0.016	
D	1.41	0	0	0.249	2
E	1.12	0	0	1.025	3
F	1.0	0	0	2.000	4
E, G	1.12	0.492	1.722	2.390	5
E, F, G	1.08	1.311	2.978	4.445	6
D, F, H	1.27	0.773	1.511	2.740	7
D, E, F, G, H	1.21	1.581	3.517	5.144	8
F, G	1.06	0.859	1.718	3.174	9
F, G, H	1.18	1.054	2.054	3.502	10
F, G, H, I, J, K	2.18	1.072	2.071	3.531	11
ALL 11	2.28	1.616	3.538	5.203	12
B, D, I	2.27	0.088	0.006	0.281	13
C, E, H	1.59	0.161	0.696	1.485	14
C, D, I	1.96	0.101	0.034	0.296	15

B_x magnetometers. B_y measurements generally have a larger V than B_x measurements, which must result from the fact that the row of magnetometers is displaced from the dipole in the y direction. Identification of the trends in the table can be simplified in Fig. 4.5 by plotting V for each type of measurement (B_x, B_y, or $\vec{B}$) as a function of the mean distance from the dipole to the measurement locations. In order to separate an increase in V due to a decrease in mean distance from one due to an increase in the number of magnetometers, the data are sorted by number of signals. For example, two B_x measurements, two B_y measurements, and one $\vec{B}$ measurement each have two signals. The graph shows several trends. For any series of measurements, V decreases with increasing mean range; the line through points 2v, 3v, and 4v has a slope of -6, consistent with Eq. 4.23 for a single vector magnetometer. Except at large mean distances, $V_{B_y} > V_{B_x}$. Whether this is true in general may depend on the choice of measurement locations. The graph also shows that high V can be obtained at large mean distances by using a large number of measurements. However, V is 5.144 for five $\vec{B}$ measurements close to the dipole, whereas adding the six more distant ones increases V only by 1%. For the 3 closest $\vec{B}$ measurements, V equals 4.445, only 14% below the value for 5 vector measurements.

The E and G sensitivity vectors for a B_y measurement were shown to be nearly perpendicular in Fig. 4.4. A simple quadradic equation can be solved to show that the B_y vectors will be perpendicular for two pairs of measurement locations: $x = \pm\ 0.56y$ and $x = \pm\ 3.56\ y$. At the first, which is close enough to be useful, $\tilde{R}$ is diagonal with equal eigenvalues and $V = 1.44$. This is plotted in Fig. 4.5 as point 16y. However, the choice of this pair of locations over E and G would depend on the relative importance of $\tilde{R}$ being diagonal versus V being 20% larger. The fact that B_y

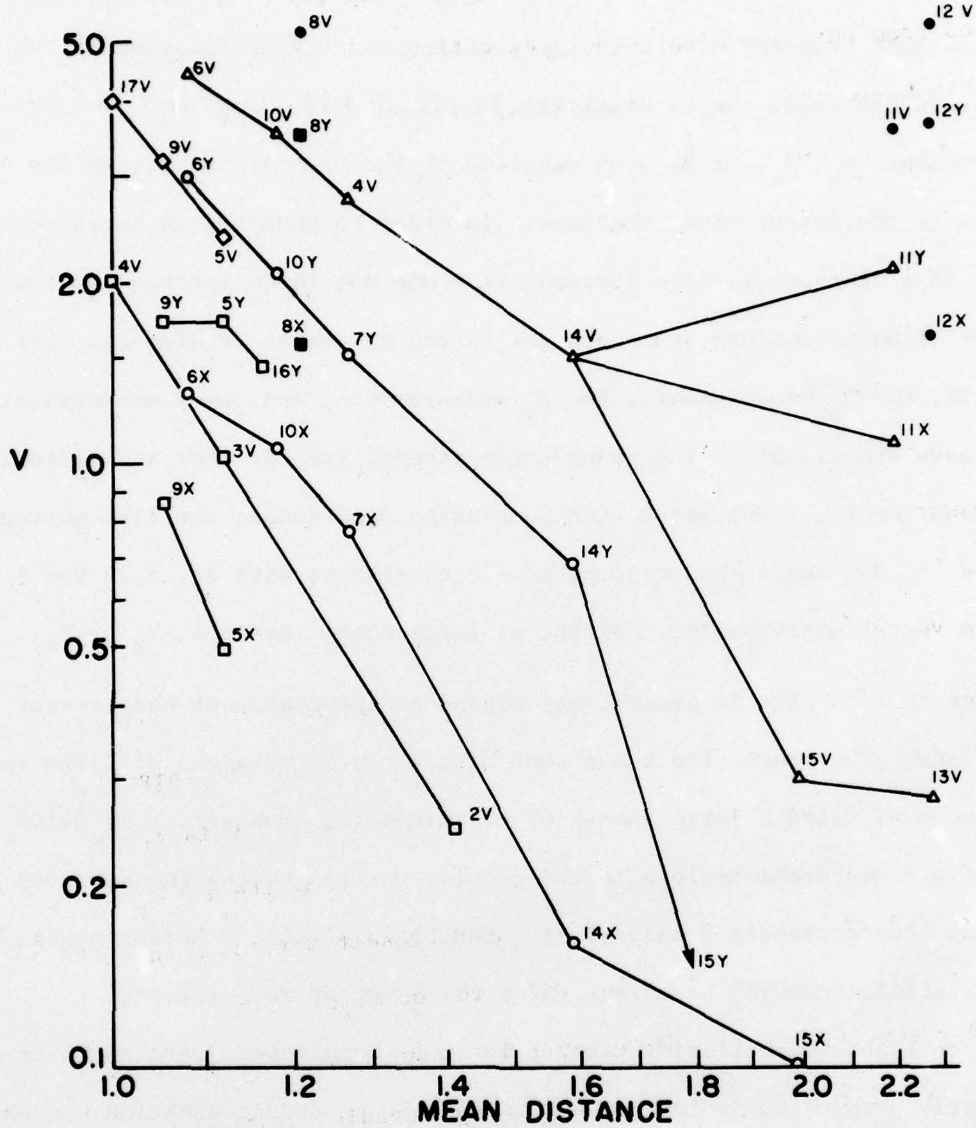

Fig. 4.5. The quantity V plotted as a function of mean distance $\bar{r}$ from the data in Table 4.4. The lines connect sets of measurements using the same type and number of magnetometers. The plot numbers are listed in Table 4.4; x, y, and v stand for B_x, B_y and $\vec{B}$ measurements. See the text for points 16y and 17v.

measurements F and G (point 9y) and measurements E and G (point 5y) have almost the same V while having x-direction separations of 0.5 and 1.0, respectively, indicates that the apparent linear relation between log V and log $\bar{r}$ doesn't necessarily hold for changes in measurement configuration in the near field region.

In Fig. 4.5, the points 5v, 9v, and 17v are for two vector magnetometers, with 17v corresponding to both magnetometers located at the same point (0.0, 1.0), for a V of 4.0. This indicates that while a large V is desired, it is possible to artificially enlarge V by repeating a measurement twice. This could be avoided by dividing V by the number of measurements taken, which would show B_x and B_y at position F to have a V/n of 1.0 and B_y at positions E, F and G to have a V/n of 0.99.

4.4 The Effects of Noise

In the preceding sections, we analyzed several different examples and studied the variation in V as a function of distance. If the measurements are affected by either external or instrument noise, then the signal at large distances will be masked by noise, so that such a measurement can not contribute fully to the modelling process. This effect can be accounted for by defining the total information matrix by

$$\tilde{R}_{TOT} = \sum_{i}^{n} w_i \tilde{R}_i \qquad (4.24)$$

where w_i is a weighting function that is zero for signals buried in noise and 1 for clean signals. For example, we can define a suitable w by

$$w_i = \frac{s_i - n_i}{s_i} = 1 - \frac{n_i}{s_i} \quad \text{for } n_i < s_i \qquad (4.25)$$

$$w_i = 0 \text{ for } n_i > s_i$$

where s_i and n_i are the signal and noise amplitude for the i^{th}

measurement. Since the magnitude of the signal is determined by both the strength of the source and the sensitivity vector for that measurement, we can replace n_i/s_i by $|\vec{N}_i|/|\vec{S}_i|$, where $\vec{N}_i$ is a noise sensitivity vector that contains the relative strength of the noise source to the signal source. The use of $|\vec{S}_i|$ is reasonable, since we showed previously that the magnitude of the sensitivity vector indicated the maximum signal from a dipole with unknown orientation. From Eq. (4.22), we find that, for a single vector magnetometer

$$\tilde{R} = \left(1 - \frac{|\vec{N}_{B_x}|}{|\vec{S}_{B_x}|}\right)\tilde{R}_{B_x} + \left(1 - \frac{|\vec{N}_{B_y}|}{|\vec{S}_{B_y}|}\right)\tilde{R}_{B_y} \qquad (4.26)$$

It follows from Eq. (3.8) that

$$|\vec{S}_{B_x}| = \frac{1}{r^4}\sqrt{4x^2 + y^2} \qquad |\vec{S}_{B_y}| = \frac{1}{r^4}\sqrt{x^2 + 4y^2} \qquad (4.27)$$

Suppose that, for a given dipolar source, the signal to noise ratio for a measurement of B_x on the y axis is unity for y = 2.0. At that point

$$1 = \frac{|\vec{N}_{B_x}|}{|\vec{S}_{B_x}|} = \frac{|\vec{N}_{B_x}|}{\frac{1}{8}} \quad \text{so} \quad |\vec{N}_{B_x}| = 0.125 \qquad (4.28)$$

If we assume that $|\vec{N}_{B_y}| = |\vec{N}_{B_x}|$, we can calculate how V for the vector measurement depends on distance along the y axis. The results, plotted in Fig. 4.6, show that at y = 1.0, V corrected for noise is 10% smaller than the original value. At y = 1.5, V is 32% smaller. At y = 0.5, the correction is only 1%.

As a final example of the addition of noise to the analysis, we stated earlier that V for a single vector magnetometer depended only on distance from the dipole. If the noise field is not the same for both B_x and B_y, i.e. $|\vec{N}_{B_x}| > |\vec{N}_{B_y}|$, then there will be an optimum magnetometer location. Continuing the previous example, let us assume that $|\vec{N}_{B_x}| = 0.250$ and $|\vec{N}_{B_y}| = 0.125$. On the x-axis, the total information matrix is given by

$$\tilde{R} = \frac{1}{x^6}\begin{pmatrix} 4(1-\frac{N_{B_x}}{2}x^3) & 0 \\ 0 & (1-N_{B_y}x^3) \end{pmatrix} \tag{4.29}$$

while that on the y-axis is

$$\tilde{R} = \frac{1}{y^6}\begin{pmatrix} (1-N_{B_x}y^3) & 0 \\ 0 & 4(1-\frac{N_{B_y}}{2}y^3) \end{pmatrix} \tag{4.30}$$

At the points (1, 0) and (0, 1), V has the values 1.75 and 1.68, respectively, compared to 1.81 when both noise sensitivities were 0.125. This is consistent with Fig. 3.2, since the larger noise in B_x can be partially offset by measuring B_x where it is the largest -- i.e. on the x-axis.

If the weighted information matrix is used in analyzing the row of magnetometers, the curves in Fig. 4.5 will be seen to fall off more quickly with mean distance. A detailed analysis of various magnetometer configurations will require realistic estimates of signal and noise strengths, to insure that $|\vec{N}_i|$ is specified correctly. Comparison of

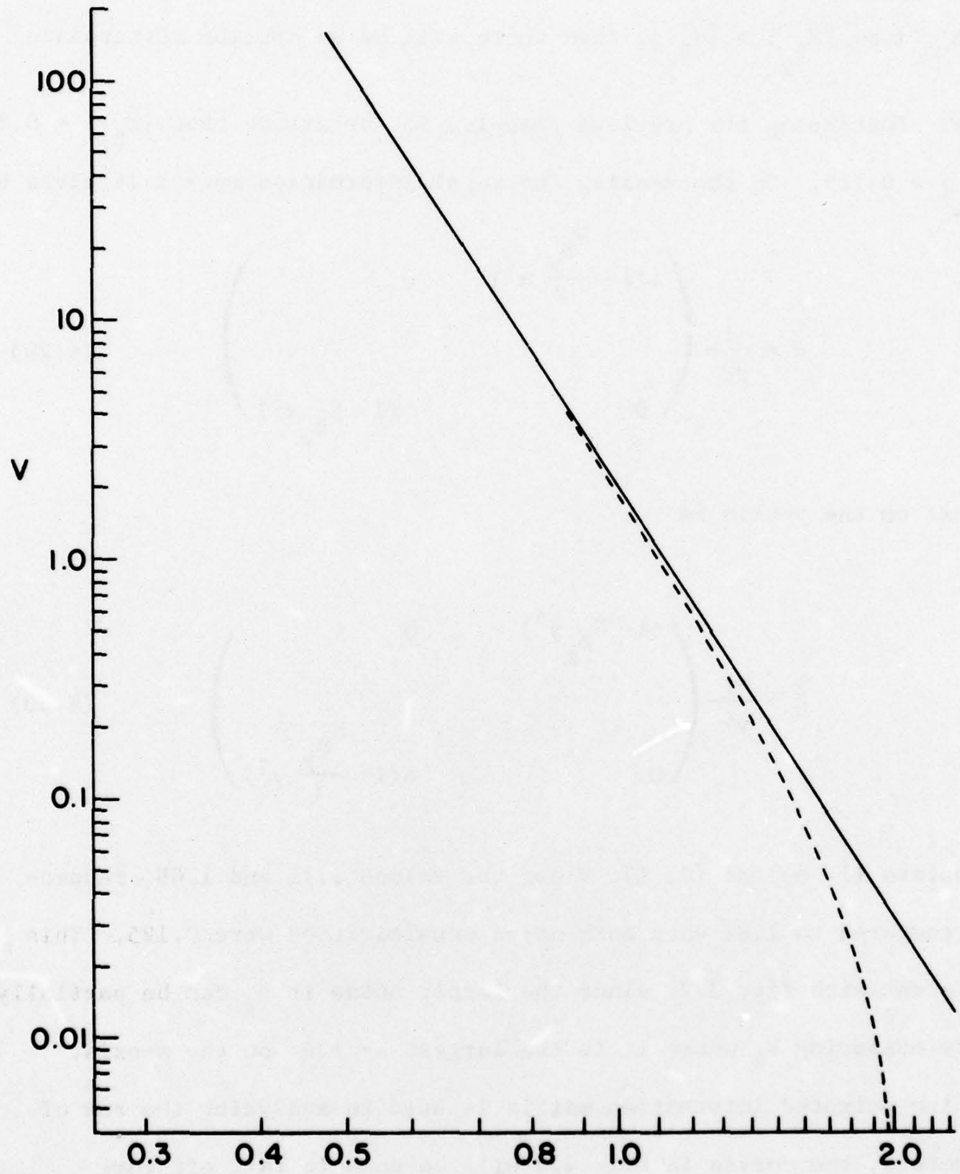

Fig. 4.6. The quantity V plotted versus y for a vector magnetometer on the y axis. The dashed line uses the noise-weighted $\tilde{R}$ while the solid one does not.

expected performance with that observed from actual field measurements might allow the use of an empirical noise weighting function, rather than given by Eq. (4.25). Thus we have developed techniques for using sensitivity vectors for analyzing and comparing various magnetometer configurations, both in the ideal noise-free case, and when noise limits the distance at which measurements can be made. Our next step is to relate this work to the reciprocity theorem prior to beginning quadrupole analysis.

V. QUADRUPOLES AND HIGHER MOMENTS

The preceeding analysis used the sensitivity vector obtained by computing the gradient of the field with respect to the model parameters. The ith measurement was shown to be given by

$$F_i = \tilde{S}_i^T \tilde{M} \tag{5.1}$$

For a dipole model, vector notation lets us write this as

$$F_i = \vec{S}_i \cdot \vec{M} \tag{5.2}$$

However, Figures 4.3 and 4.4 showed that the components of these sensitivity vectors have the same spatial dependence as the field of a dipole. This and Eq. (5.2) are simply demonstrations of the reciprocity theorem, which will be shown to provide the basis for interpreting the sensitivity of a magnetometer to magnetic quadrupoles and higher order moments.

5.1 The Sensitivity of a Magnetometer to a Distributed Magnetization

We have considered the magnetic field produced by a point magnetic dipole

$$\vec{B}(\vec{r}) = \frac{\mu_o}{4\pi}\left(\frac{3\vec{m}\cdot(\vec{r}-\vec{r}\,')(\vec{r}-\vec{r}\,')}{|\vec{r}-\vec{r}\,'|^5} - \frac{\vec{m}}{|\vec{r}-\vec{r}\,'|^3}\right) \tag{5.3}$$

For a source which is a distributed magnetization, we can identify the magnetization $\vec{M}(\vec{r})$ as a magnetic dipole density and integrate Eq. (5.3) over the source volume to obtain

$$\vec{B}(\vec{r}) = \frac{\mu_o}{4\pi}\int_V \left[\frac{3\vec{M}(\vec{r}\,')\cdot(\vec{r}-\vec{r}\,')(\vec{r}-\vec{r}\,')}{|\vec{r}-\vec{r}\,'|^5} - \frac{\vec{M}(\vec{r}\,')}{|\vec{r}-\vec{r}\,'|}\right] d^3r' \tag{5.4}$$

Alternatively, the field can be determined by noting that

$$\vec{B}(\vec{r}) = -\nabla\phi(\vec{r}) \tag{5.5}$$

with ϕ being described by the traceless tensor multipole expansion listed in Table 5.1. The separation of the source into dipole, quadrupole and higher moments is ideal for modelling, and we thus see the need for expressions describing the sensitivity vectors that relate a field measurement to each multipole moment. Based on our previous discussion, we could compute the gradient of each potential term in Table 5.1 to obtain the corresponding contribution to $\vec{B}$, and then compute the gradient of each $\vec{B}$ with respect to the moment to obtain the sensitivity vector. Rather than do this, we will use the magnetic vector potential $\vec{A}$ to derive an expression equivalent to Eq. (5.4) This expression will help explain the physical significance of sensitivity vectors.

If we represent a single axis magnetometer by a small pick-up loop, then the magnetometer output will be proportional to the flux ϕ coupling the magnetometer, given by

$$\Phi = \int \vec{B}(r) \cdot \vec{da} \tag{5.6}$$

where $\vec{da}$ is the normal to an element of surface bounded by the loop. Because $\nabla \cdot \vec{B} = 0$, we can write

$$\vec{B}(r) = \nabla \times \vec{A}(\vec{r}) \tag{5.7}$$

so that

$$\Phi = \int \nabla \times \vec{A}(r) \cdot \vec{da} \tag{5.8}$$

Stoke's Theorem can be used to convert this to the line integral

$$\Phi = \oint \vec{A}(\vec{r}) \cdot \vec{d\ell} \tag{5.9}$$

where $\vec{d\ell}$ is a length element of the pick-up coil system. We now need to

TABLE 5.1

The Traceless Tensor Multipole Expansion for a Distributed Magnetization

$$\phi(r) = \sum_{i=1}^{3} m_i \phi_i + \sum_{i=1}^{3} \sum_{j=1}^{3} Q_{ij} \phi_{ij} + \ldots$$

DIPOLE

$$\phi_i = \frac{1}{4\pi^3} \frac{x_i}{r^3} \qquad m_i = \int_V M(\vec{r}\,')\, d^3r'$$

QUADRUPOLE

$$\phi_{xx} = \frac{1}{4\pi} \frac{3x^2 - r^2}{2r^5} \qquad Q_{xx} = \int_V \left[2x' M_x(\vec{r}\,') - \frac{2}{3} \vec{r} \cdot \vec{M}(\vec{r}\,') \right] d^3r'$$

$$\phi_{yy} = \frac{1}{4\pi} \frac{3y^2 - r^2}{2r^5} \qquad Q_{yy} = \int_V \left[2y' M_y(\vec{r}\,') - \frac{2}{3} \vec{r} \cdot \vec{M}(\vec{r}\,') \right] d^3r'$$

$$\phi_{zz} = \frac{1}{4\pi} \frac{3z^2 - r^2}{2r^5} \qquad Q_{zz} = \int_V \left[2z' M_z(\vec{r}\,') - \frac{2}{3} \vec{r} \cdot \vec{M}(\vec{r}\,') \right] d^3r'$$

$$\phi_{xy} = \phi_{yx} = \frac{1}{4\pi} \frac{3xy}{2r^5} \qquad Q_{xy} = Q_{yx} = \int_V \left[x' M_y(\vec{r}\,') - y' M_x(\vec{r}\,') \right] d^3r'$$

$$\phi_{yz} = \phi_{zy} = \frac{1}{4\pi} \frac{3yz}{2r^5} \qquad Q_{yz} = Q_{zy} = \int_V \left[y' M_z(\vec{r}\,') - z' M_y(\vec{r}\,') \right] d^3r'$$

$$\phi_{xz} = \phi_{zy} = \frac{1}{4\pi} \frac{3xz}{2r^5} \qquad Q_{xz} = Q_{zx} = \int_V \left[x' M_z(\vec{r}\,') - z' M_x(\vec{r}\,') \right] d^3r'$$

relate $\vec{A}$ to $\vec{M}$, and do this by starting with Maxwell's fourth equation

$$\nabla \times \vec{B} = \mu_o \nabla \times \vec{M} \tag{5.10}$$

which becomes

$$\nabla \times (\nabla \times \vec{A}) = \mu_o(\nabla \times \vec{M}) \tag{5.11}$$

But the vector identity $\nabla \times (\nabla \times \vec{A}) = \nabla(\nabla \cdot \vec{A}) - \nabla^2\vec{A}$ lets us write

$$\nabla^2 A = \nabla(\nabla \cdot \vec{A}) - \mu_o(\nabla \times \vec{M}) \tag{5.12}$$

The Coulomb gauge can be chosen to set the first term on the right to zero, leaving

$$\nabla^2 A(\vec{r}) = -\mu_o(\nabla \times \vec{M}(\vec{r})) \tag{5.13}$$

which is Poisson's equation. In cartesian coordinates, the solution is

$$\vec{A}(\vec{r}) = \frac{\mu_o}{4\pi} \int_V \frac{\nabla' \times \vec{M}(\vec{r}\,')}{|\vec{r} - \vec{r}\,'|} d^3r' \tag{5.14}$$

The vector identity $V\nabla \times \vec{U} = \nabla \times (V\vec{U}) - \nabla V \times \vec{U}$ can be used to rewrite this as

$$\vec{A}(\vec{r}) = \frac{\mu_o}{4\pi} \int_V \nabla' \times \frac{\vec{M}(\vec{r}\,')}{|\vec{r} - \vec{r}\,'|} d^3r - \frac{\mu_o}{4\pi} \int_V \nabla'\left(\frac{1}{|\vec{r} - \vec{r}\,'|}\right) \times \vec{M}(\vec{r}\,')d^3r \tag{5.15}$$

The first volume integral can be converted into a surface integral that vanishes for any bounded magnetization distribution. Therefore

$$\vec{A}(\vec{r}) = \frac{\mu_o}{4\pi} \int_V \vec{M}(\vec{r}\,') \times \nabla'\left(\frac{1}{|\vec{r} - \vec{r}\,'|}\right)d^3r \tag{5.16}$$

Substituting this into Eq. (5.9), we find

$$\Phi = \frac{\mu_o}{4\pi}\oint\int\int_V \left[\vec{M}(\vec{r}\,') \times \nabla'\left(\frac{1}{|\vec{r} - \vec{r}\,'|}\right) d^3r'\right] \cdot \vec{d\ell} \tag{5.17}$$

The terms of the scalar triple product can be permuted and the order of integration reversed to obtain

$$\Phi = \frac{\mu_o}{4\pi}\int_V \left[\nabla' \times \oint \frac{\vec{d\ell}}{|\vec{r} - \vec{r}\,'|}\right] \cdot \vec{M}(\vec{r}\,')\, d^3r' \tag{5.18}$$

Recall that a test current I_p flowing in the pick-up coil has a vector potential

$$\vec{A}_p(\vec{r}\,') = \frac{\mu_o I_p}{4\pi}\oint \frac{\vec{d\ell}}{|\vec{r} - \vec{r}\,'|} \tag{5.19}$$

associated with a magnetic field

$$\vec{B}_p(\vec{r}\,') = \nabla' \times \vec{A}_p(\vec{r}\,') \tag{5.20}$$

With this identification, we may write Eq. (5.18) as

$$\Phi = \frac{1}{I_p}\int_V \vec{B}_p(\vec{r}\,') \cdot \vec{M}(\vec{r}\,')\, d^3r' \tag{5.21}$$

Thus we see that for an arbitrary pick-up loop configuration, the contribution to the magnetometer output from a source element at $\vec{r}\,'$ can be determined from the magnetic field $\vec{B}_p$ produced at $\vec{r}\,'$ by passing a test current I_p through the pick-up coil. The reversal of the order of integration prior to Eq. (5.18) and the identification of the line integral in Eq. (5.19) are simply a statement of the electromagnetic reciprocity theorem. Comparison of Eqs. (5.2) and (5.21) results in this identification:

> At a given source location, the sensitivity vector for a single axis magnetometer is equivalent to the magnetic field produced at that location by passing a unit test current through the magnetometer pick-up coil.

Since the magnetometers used in Fig. 4.3 and 4.4 were assumed to be small, it is correct that their field $\vec{B}_p$ would be dipolar. Interpretation of Fig. 3.1 is also straightforward. The sensitivity vector for each B_x magnetometer location corresponds to the magnetic field produced at the origin by passing a test current through the magnetometer.

Equation (5.21), with its simple interpretation, provides the key for understanding the sensitivity to higher moments: the integrand $\vec{B}_p(\vec{r}') \cdot \vec{M}(\vec{r}')$ can be broken down into various multipole terms using a Taylor's expansion of $\vec{B}_p(\vec{r}')$ and a multipole expansion of $\vec{M}(\vec{r}')$, so that $\vec{B}_p$ represents the sensitivity to the dipole component $\vec{m}$, each spatial gradient of $\vec{B}_p$ represents the sensitivity to the corresponding quadrupole moments and so forth. If the magnetometer is a simple scalar instrument, $\vec{B}_p$ can be obtained from Eq. (2.3), where $\hat{m}_p$ is the unit dipole moment produced by I_p. For a B_x magnetometer, $\hat{m}_p = \hat{i}$. For a gradient magnetometer, $\vec{B}_p(\vec{r})$ will be characteristic of a magnetic quadrupole, but the sensitivity of this instrument to a magnetic dipole will still be given by $\vec{B}_p \cdot \vec{m}$.

Based on this discussion, we will proceed to determine the sensitivity of a vector magnetometer to a dipole-plus-quadrupole source. Calculation of the components of $\vec{B}_p$ is straightforward. There are nine gradients of $\vec{B}_p$ that can be written as a gradient tensor

$$\begin{pmatrix} \frac{\partial B_x}{\partial x} & \frac{\partial B_y}{\partial x} & \frac{\partial B_z}{\partial x} \\ \frac{\partial B_x}{\partial y} & \frac{\partial B_y}{\partial y} & \frac{\partial B_z}{\partial y} \\ \frac{\partial B_x}{\partial z} & \frac{\partial B_y}{\partial z} & \frac{\partial B_z}{\partial z} \end{pmatrix} \tag{5.22}$$

Just as the quadrupole tensor in Table 5.1 is traceless and symmetric, the condition that $\nabla \times \vec{B}_p$ is zero in a current-free region implies that the gradient tensor for $\vec{B}_p$ is symmetric, so that we can write the $\vec{B}_p$ gradient tensor as

$$\begin{pmatrix} \frac{\partial B_x}{\partial x} & \frac{\partial B_y}{\partial x} & \frac{\partial B_z}{\partial x} \\ \frac{\partial B_y}{\partial x} & \frac{\partial B_y}{\partial y} & \frac{\partial B_z}{\partial y} \\ \frac{\partial B_z}{\partial x} & \frac{\partial B_z}{\partial y} & \frac{\partial B_z}{\partial z} \end{pmatrix} \tag{5.23}$$

The condition that $\nabla \cdot \vec{B}_p = 0$ implies that this tensor is also traceless. We can therefore omit both $\partial B_z/\partial z$ and Q_{zz} from our discussion, since they can be derived from the other two terms of each trace.

The following pairs of quantities will be required for the sensitivity analysis

$$\text{DIPOLE} \begin{cases} 1: & B_x \ , \ m_x \\ 2: & B_y \ , \ m_y \\ 3: & B_z \ , \ m_z \end{cases} \tag{5.24}$$

(5.24 cont'd)

$$\text{QUADRUPOLE}\left\{\begin{array}{ll} 4: & \dfrac{\partial B_x}{\partial x}\ ,\ Q_{xx} \\[2ex] 5: & \dfrac{\partial B_y}{\partial y}\ ,\ Qyy \\[2ex] 6: & \dfrac{\partial B_y}{\partial x}\ ,\ Q_{xy} \\[2ex] 7: & \dfrac{\partial B_z}{\partial x}\ ,\ Q_{xz} \\[2ex] 8: & \dfrac{\partial B_z}{\partial y}\ ,\ Q_{yz} \end{array}\right.$$

The terms on the right correspond to the eight axes in model space, while the quantities on the left correspond to the eight components of each sensitivity vector. If each set of eight quantities is thought of as a (1 x 8) matrix or an 8-vector, then the magnetometer output corresponds to the inner (scalar) product of these two matrices (vectors). In computing the gradients of $\vec{B}_p$ using Eq. (2.3), it is important to note that $\vec{r}'$ is the location of the pick-up coil and $\vec{r}$ is the location of the model, and the gradients are computed with respect to the source location. The sign of I_p (or $\hat{m}_p$) can be chosen to insure, for example, that Q_{xx} as shown in Fig. 5.1 will produce a positive B_x on the positive x-axis.

The eight sensitivity vector components for each of the vector magnetometer axes are listed in Table 5.2. These results, which were obtained by computing the appropriate gradients of $\vec{B}_p$, could also be obtained by computing the appropriate gradients of the potentials in Table 5.1. Comparison of the two methods shows that a factor of $\mu_o/4\pi$ must multiply each term in Table 5.2 to provide the proper units, and an additional factor of 1/2 must multiply the quadrupole terms to provide a

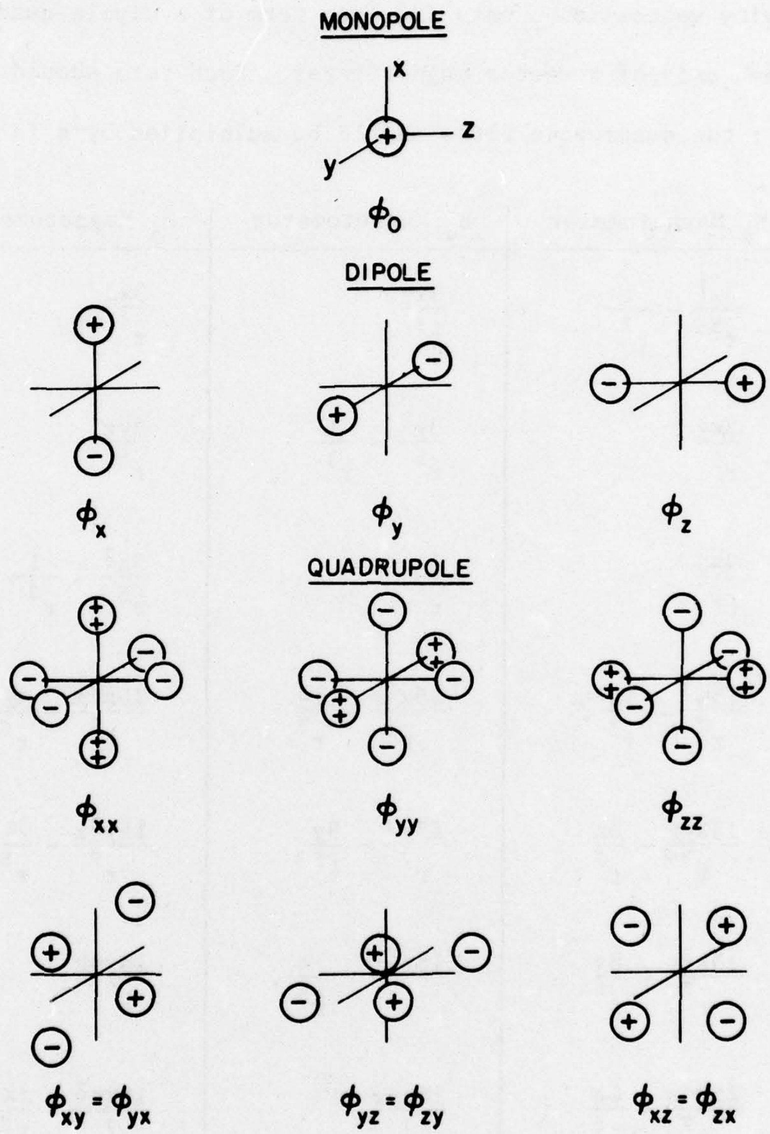

Fig. 5.1. The source-sink pictures for the dipole and quadrupole in the traceless tensor representation.

TABLE 5.2

The sensitivity vector components for each term of a dipole-quadrupole model and each axis of a vector magnetometer. Each term should be multiplied by $\frac{\mu_o}{4\pi}$; the quadrupole terms should be multiplied by a factor of ½.

	B_x Magnetometer	B_y Magnetometer	B_z Magnetometer
m_x	$\frac{3x^2}{r^5} - \frac{1}{r^3}$	$\frac{3xy}{r^5}$	$\frac{3xz}{r^5}$
m_y	$\frac{3xy}{r^5}$	$\frac{3y^2}{r^5} - \frac{1}{r^3}$	$\frac{3yz}{r^5}$
m_z	$\frac{3xz}{r^5}$	$\frac{3yz}{r^5}$	$\frac{3z^2}{r^5} - \frac{1}{r^3}$
Q_{xx}	$\frac{15x^3}{r^7} - \frac{9x}{r^5}$	$\frac{15x^2y}{r^7} - \frac{3y}{r^5}$	$\frac{15x^2z}{r^7} - \frac{3z}{r^5}$
Q_{yy}	$\frac{15xy^2}{r^7} - \frac{6x}{r^5}$	$\frac{15y^3}{r^7} - \frac{9y}{r^5}$	$\frac{15y^2z}{r^7} - \frac{3z}{r^5}$
Q_{xy}	$\frac{15x^2y}{r^7} - \frac{6y}{r^5}$	$\frac{15xy^2}{r^7} - \frac{3x}{r^5}$	$\frac{15xyz}{r^7}$
Q_{xz}	$\frac{15x^2z}{r^7} - \frac{6z}{r^5}$	$\frac{15xyz}{r^7}$	$\frac{15xz^2}{r^7} - \frac{3x}{r^5}$
Q_{yz}	$\frac{15xyz}{r^7}$	$\frac{15y^2z}{r^7} - \frac{3z}{r^5}$	$\frac{15yz^2}{r^7} - \frac{3y}{r^5}$

TABLE 5.3

The sensitivity vector components for each axis of a vector magnetometer located at the points (1, 0, 0), (0, 1, 0) and (0, 0, 1) obtained from the equations in Table 5.2.

	(1, 0, 0)			(0, 1, 0)			(0, 0, 1)		
	B_x	B_y	B_z	B_x	B_y	B_z	B_x	B_y	B_z
m_x	2	0	0	-1	0	0	-1	0	0
m_y	0	-1	0	0	2	0	0	-1	0
m_z	0	0	-1	0	0	-1	0	0	2
Q_{xx}	6	0	0	0	-6	0	0	0	-6
Q_{yy}	-6	0	0	0	6	0	0	0	-6
Q_{xy}	0	-6	0	-6	0	0	0	0	0
Q_{xz}	0	0	-6	0	0	0	-6	0	0
Q_{yz}	0	0	0	0	0	-6	0	-6	0

correct Taylor's expansion of $\vec{B}_p$.

Table 5.3 lists the sensitivity vector components for vector magnetometers a unit distance from the source along the positive x, y, and z axes. It is important to note from the table that Q_{yz} does not affect $\vec{B}(1, 0, 0)$, while Q_{xz} and Q_{yz} do not affect $\vec{B}(0, 1, 0)$ and $\vec{B}(0, 0, 1)$, respectively. This is in contrast to the single dipole case discussed previously, in which the invertability of the field equations was dependent only upon distance from the source. Table 5.3 can also be used to clarify the orientation of the field from each quadrupole in Fig. 5.1.

Given the sensitivity vector equations in Table 5.2, the previous numerical examples can be readily extended to include the quadrupole terms. However, the information matrix will then be (8 x 8), which can be manipulated most efficiently with a digital computer and thus will not be addressed further in this report.

VI. NONLINEAR PROBLEMS

In all of the models discussed so far, the field equations were linear with respect to the source parameters. For this reason, the computation of the sensitivity vectors was simple, and the results were consistent with the reciprocity theorem. If we had chosen the position of the dipole as a model parameter, the three components of r' in Eq. (2.3) would represent three non-linear terms in the field equation. We will now proceed to extend our sensitivity vector techniques to include this case.

6.1 Taylor's Series Linearization

In section II, we showed that for linear systems the fields and model are related by an equation of the form

$$\tilde{F} = \tilde{T}\,\tilde{M} \tag{6.1}$$

where $\tilde{F}$ is an n x 1 matrix, $\tilde{M}$ is an m x 1 matrix, and $\tilde{T}$ is m x n. In the non-linear case, we can write

$$\tilde{F} = \tilde{f}(\tilde{M}) \tag{6.2}$$

where $\tilde{f}(\tilde{M})$ represents a set of n non-linear functions of the m model parameters. For example, each equation in $\tilde{f}$ could be a different polynomial. If we choose a point in model space $\tilde{M}^o$ and determine the corresponding point in field space $\tilde{F}^o$

$$\tilde{F}^o = \tilde{f}(\tilde{M}^o) \tag{6.3}$$

If we restrict ourselves to the point $\tilde{M}^o$, we can write this as

$$\tilde{F}^o = \tilde{T}^o\,\tilde{M}^o \tag{6.4}$$

We can then approximate $\tilde{f}$ in a region about this point using a Taylor's series expansion of each of the n equations in $\tilde{f}$. In matrix notation, these can be written as

$$\tilde{F} = \tilde{f}(\tilde{M})$$

$$= \tilde{f}(\tilde{M}_o) + \sum_j \frac{\partial \tilde{f}(\tilde{M}^o)}{\partial M_j} (M_j - M_j^o) + \ldots \qquad (6.5)$$

The summation containing the partial derivative can be represented by a matrix multiplication, so that the equation reduces to

$$\tilde{F} = \tilde{F}^o + \tilde{J}(\tilde{M}^o)(\tilde{M} - \tilde{M}^o) + \ldots \qquad (6.6)$$

where $\tilde{J}(\tilde{M}^o)$ is the Jacobian matrix $\tilde{J}(\tilde{M})$ evaluated at $\tilde{M}^o$, with

$$\tilde{J}(\tilde{M}) = \begin{vmatrix} \frac{\partial f_1}{\partial M_1} & \ldots & \frac{\partial f_1}{\partial M_m} \\ \cdot & & \cdot \\ \cdot & & \cdot \\ \cdot & & \cdot \\ \frac{\partial f_n}{\partial M_1} & \ldots & \frac{\partial f_n}{\partial M_m} \end{vmatrix} \qquad (6.7)$$

The right hand side of Eq. (6.5) is a linear vector function of $\tilde{M}$ which best approximates the non-linear function $\tilde{f}(\tilde{M})$ at the point $\tilde{M}^o$. This linear function describes the tangent hyperplane to the surface $\tilde{F} = \tilde{f}(\tilde{M})$ at $\tilde{M}^o$.

If we know $\tilde{F}$ from a series of measurements and wish to determine the corresponding $\tilde{M}$, it is necessary to solve Eq. (6.2). One way to do this is make a trial guess for $\tilde{M}$, say $\tilde{M}^o$, and use Eq. (6.3) to compute $\tilde{F}^o$. The error in the fields can be written as

$$\Delta\tilde{F} = \tilde{F} - \tilde{F}^o \qquad (6.8)$$

From Eq. (6.6), the error in the model is given by

$$\Delta\tilde{M} = \tilde{M} - \tilde{M}^{o} \simeq \tilde{J}(\tilde{M}^{o})^{-1} \; \Delta\tilde{F} \tag{6.9}$$

The choice of the point for computing the Taylor's series can be changed to $\tilde{M}^{1} = \tilde{M}^{o} + \Delta\tilde{M}$ and the process repeated iteratively to obtain the desired accuracy. Of course, problems will occur if the Jacobian matrix is non-invertable or if the choice of $\tilde{M}^{o}$ leads to a phantom solution.

6.2 Sensitivity Vectors for Non-Linear Systems

If we compare Eq. (6.5) with Eq. (2.7) which defined sensitivity vectors, we see that

$$F_i = F_i^{\,o} + \sum_{j=1}^{m} \frac{\partial f_i}{\partial M_j} \; (M_j - M_j^{\,o}) + \ldots \tag{6.10}$$

$$\simeq F_i^{\,o} + \sum_{j=1}^{m} (\tilde{S}_i)_j \; (M_j - M_j^{\,o}) \tag{6.11}$$

which by Eqs. 6.8 and 6.9 becomes

$$\Delta F_i \simeq \tilde{S}_i^{\,T} \; \Delta\tilde{M} \tag{6.12}$$

Using Eq. (6.4) instead of F^{o}, we could also have written Eq. (6.11) as

$$F_i \simeq \sum_{j=1}^{m} T_{ij}^{\;o} \, M_j^{\,o} + \tilde{S}_i^{\,T} \; (\tilde{M} - \tilde{M}^{o}) \tag{6.13}$$

It is apparent that the sensitivity vectors no longer correspond to the rows of $\tilde{T}$, but instead to the rows of the Jacobian matrix.

The derivations of Section IV can be repeated to relate this to the information matrix. Multiplying Eq. 6.12 by $\tilde{S}_i$ and summing over all measurements, we obtain

$$\sum_{i=1}^{n} \tilde{S}_i \, \Delta F_i = \sum_{i=1}^{n} \tilde{S}_i \, \tilde{S}_i^T \, \widetilde{\Delta M} \tag{6.14}$$

This can be solved for $\widetilde{\Delta M}$

$$\widetilde{\Delta M} \simeq \left(\sum_{i=1}^{n} \tilde{S}_i \, \tilde{S}_i^T \right)^{-1} \sum_{i=1}^{n} \tilde{S}_i \, \Delta \tilde{F}_i \tag{6.15}$$

Using Eq. (6.11), we can also write

$$\tilde{M} \simeq \tilde{M}^o + \tilde{R}^{-1} \sum_{i=1}^{n} \tilde{S}_i \, (F_i - F_i^{\,o}) \tag{6.16}$$

This equation, which uses sensitivity vectors and the information matrix, represents the solution of the linearized version of our original non-linear field equation.

Thus we see that even with non-linear systems, sensitivity vectors have a straightforward mathematical interpretation. As in the linear case, their utility lies in their simple physical interpretation in terms of measurement sensitivity and in their suitability for graphical presentation. It is important to recognize that in practice, sensitivity vectors can be determined either analytically or numerically. If we have a measurement that is a linear function of some variables and a non-linear function of several others, we can use the sensitivity vector approach to determine how the measurement is affected by each variable, regardless of whether the variable has a linear or non-linear effect on the measurement. However, we have just shown that the interpretation does depend somewhat on whether the dependence is linear or non-linear. If the i^{th} measurement is described by F_i, it follows from our original definitions that <u>for the linear case</u>, the sensitivity vector for this measurement is

$$\vec{S}_i = \nabla_M F_i \tag{6.17}$$

and that

$$F_i = \vec{S}_i \cdot \vec{M} \tag{6.18}$$

Because of the linear relationship, the change in the measurement resulting from a change in the model is simply

$$\Delta F_i = \vec{S}_i \cdot \overrightarrow{\Delta M} \quad \begin{pmatrix} \text{linear case,} \\ \text{any } \Delta\vec{M} \end{pmatrix} \tag{6.19}$$

In the non-linear case, the sensitivity vectors is still given by Eq. (6.17), but we have shown that Eq. (6.18) does not apply, and that (6.19) <u>does</u> apply as long as higher order terms can be neglected. Thus we can write

$$\Delta F_i = \vec{S}_i \cdot \overrightarrow{\Delta M} \quad \begin{pmatrix} \text{non-linear case,} \\ \text{small } \Delta\vec{M} \end{pmatrix} \tag{6.20}$$

This leads us to the important conclusion

> If sensitivity vectors are interpreted as a measure of how a measurement is affected by a <u>small</u> change in the model, then linear and non-linear problems can be treated identically.

6.3 The Sensitivity of a Vector Magnetometer to Dipole Position

As a non-linear example of sensitivity vectors, we will extend our previous example and determine the sensitivity of a vector magnetometer to small changes in the location of the dipole. The sensitivity of B_x to changes in dipole location can be determined by computing the gradient of $B_x(\vec{r})$, given by Eq. (2.4), with respect to $\vec{r}'$. The resulting sensitivity vector is

$$\vec{S}(B_x) = \frac{\partial B_x(\vec{r})}{\partial x'}\hat{i}' + \frac{\partial B_x(\vec{r})}{\partial y'}\hat{j}' \tag{6.21}$$

This can be combined with the sensitivity vector for the dipole components, to obtain

$$\begin{aligned}\vec{S}(B_x) &= \frac{\partial B_x(\vec{r})}{\partial m_x}\hat{i} + \frac{\partial B_x(\vec{r})}{\partial m_y}\hat{j} + \frac{\partial B_x(\vec{r})}{\partial x'}\hat{i}' + \frac{\partial B_x(\vec{r})}{\partial y'}\hat{j}' \\ &= S_1\hat{i} + S_2\hat{j} + S_3\hat{i}' + S_4\hat{j}'\end{aligned} \tag{6.22}$$

The analytic expressions for these sensitivity vector components, as well as the corresponding ones for B_y, are listed in Table 6.1. It is important to note from Eq. (2.3) that the gradient of $\vec{B}$ with respect to $\vec{r}$ is equal, with opposite sign, to the gradient with respect to $\vec{r}'$. Thus S_3 and S_4 also describe, if multipled by -1, the change in the measurement produced by a small change in the magnetometer location.

The equations for S_3 and S_4 indicate that the position sensitivity at a particular location depends upon the dipole components. For this reason, we must choose $\vec{m}$ for example of position sensitivity. As an extension of Table 3.3 and Figure 3.2, Table 6.2 lists B_x, B_y, the corresponding values of S_3 and S_4, and the quantity V_{34} for 2 dipole orientations, where

$$V_{34} = |S_3(B_x)S_4(B_y) - S_3(B_y)S_4(B_x)| \tag{6.23}$$

Comparison of the $\vec{m} = (1, 0)$ data for locations A and E shows that a vector

TABLE 6.1

The four components of the sensitivity vectors of B_x and B_y magnetometers that describe how B_x and B_y are affected by small changes in the components and position of a dipole located at the origin.

$$S_1(B_x) = \frac{\partial B_x}{\partial m_x} = \frac{1}{r^5}(3x^2 - r^2)$$

$$S_2(B_x) = \frac{\partial B_x}{\partial m_y} = \frac{1}{r^5}(3xy)$$

$$S_3(B_x) = \frac{\partial B_x}{\partial x'} = \frac{1}{r^7}\left[m_x(6x^3 - 9xy^2) + m_y(12x^2y - 3y^3)\right]$$

$$S_4(B_x) = \frac{\partial B_x}{\partial y'} = \frac{1}{r^7}\left[m_x(12x^2y - 3y^3) + m_y(-3x^3 + 12xy^2)\right]$$

$$S_1(B_y) = \frac{\partial B_y}{\partial m_x} = \frac{1}{r^5}(3xy)$$

$$S_2(B_y) = \frac{\partial B_y}{\partial m_y} = \frac{1}{r^5}(3y^2 - r^2)$$

$$S_3(B_y) = \frac{\partial B_y}{\partial x'} = \frac{1}{r^7}\left[m_x(12x^2y - 3y^3) + m_y(-3x^3 + 12xy^2)\right]$$

$$S_4(B_y) = \frac{\partial B_y}{\partial y'} = \frac{1}{r^7}\left[m_x(-3x^3 + 12xy^2) + m_y(-9x^2y + 6y^3)\right]$$

TABLE 6.2

The position sensitivity vectors S_3 and S_4 of B_x and B_y measurements for two dipole orientations.

Measurement Location	Coordinate	m_x	m_y	B_x	$S_3(B_x)$	$S_4(B_x)$	B_y	$S_3(B_y)$	$S_4(B_y)$	V_{34}
A	1.00, 0.00	1	0	2.00	6.00	0.00	0.00	0.00	-3.00	18.0
B	0.92, 0.38	1	0	1.56	3.48	3.75	1.06	3.75	-0.74	15.5
C	0.71, 0.71	1	0	0.50	-1.07	3.22	1.50	3.22	3.22	13.8
D	0.38, 0.92	1	0	-0.56	-2.57	-0.74	1.06	-0.74	3.75	6.6
E	0.00, 1.00	1	0	-1.00	0.00	-3.00	0	-3.00	0.00	9.0
A	1.00, 0.00	0	1	0	0.00	-3.00	-1.00	-3.00	0.00	9.0
B	0.92, 0.38	0	1	1.06	3.75	-0.74	-0.56	-0.74	-2.57	6.6
C	0.71, 0.71	0	1	1.50	3.22	3.22	0.50	3.22	-1.07	13.8
D	0.38, 0.92	0	1	1.06	-0.74	3.75	1.56	3.75	3.48	15.5
E	0.00, 1.00	0	1	0	-3.00	0.00	2.00	0.00	6.00	18.0

field measurement is twice as sensitive ($V_{34} = 18$) to changes in dipole position for measurements on the dipole axis than for equidistance measurements perpendicular to the dipole axis ($V_{34} = 9$). The position sensitivity is even lower at point D ($V_{34} = 6.0$). The relationship of the position sensitivity vectors for B_x and B_y measurements is shown graphically in Fig. 6.1.

While S_3 and S_4 follow directly from the slope of B_x vs x, B_x vs y, B_y vs x and B_y vs y signatures passing through each measurement point, the orientation of the position sensitivity vectors follows more directly from another type of plot. From Eq. (6.20), the change in field associated with a change in position will be

$$\begin{aligned} \Delta B_i &= \vec{S}_i \cdot \overrightarrow{\Delta M}_i = S_3 \Delta x' + S_4 \Delta y' \\ &= \nabla' \; B_i(\vec{r}) \cdot \overrightarrow{\Delta r}' \qquad (6.24) \\ &= \nabla B_i \cdot \overrightarrow{\Delta r} \end{aligned}$$

Thus any displacement of the magnetometer parallel to a line of constant B_i will produce no change in field. A corresponding displacement in the source will also produce no change. By identifying the sensitivity vector S_i with the spatial gradient of B_i, we see immediately that S_i must be perpendicular to lines of constant B_i. Given that

$$B_x = \frac{\mu_o}{4\pi} \frac{m(2x^2 - y^2)}{r^5} \qquad B_y = \frac{\mu_o}{4\pi} \frac{3mxy}{r^5} \qquad (6.25)$$

it follows from the parametric substitution $y = \alpha x$ that the lines of constant B_x must satisfy the equations

$$x = \left(\frac{1}{B_x} \frac{\mu_o}{4\pi} \frac{m(2 - \alpha^2)}{(1 + \alpha^2)^{5/2}} \right)^{1/3}, \qquad y = \alpha x \qquad (6.26)$$

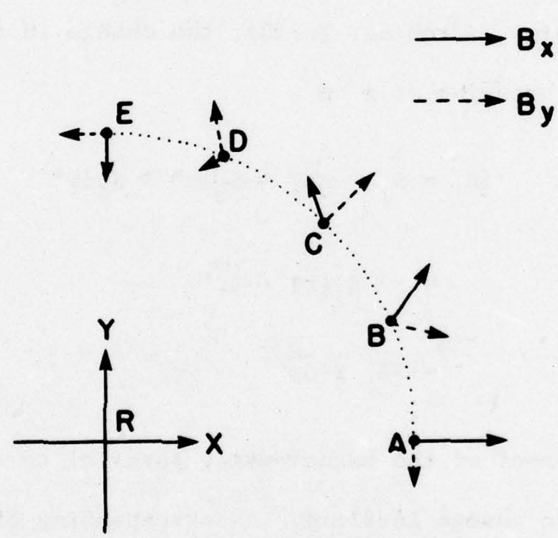

Fig. 6.1 The position sensitivity vectors for measurements of B_x and B_y at unit distance from a magnetic dipole located near the origin and parallel to the x-axis. The data are obtained from Table 6.2.

while those for B_y must satisfy

$$x = \left(\frac{1}{B_y} \frac{\mu_o}{4\pi} \frac{m(3\alpha)}{(1+\alpha^2)^{5/2}} \right)^{1/3} , \qquad y = \alpha x \tag{6.27}$$

The lines where the magnitude of $\vec{B}$ is constant satisfy

$$x = \left(\frac{m}{|\vec{B}|} \frac{\mu_o}{4\pi} \right)^{1/3} \left(\frac{4+\alpha^2}{(1+\alpha^2)^4} \right)^{1/6} , \qquad y = \alpha x \tag{6.28}$$

One set of iso-B_x lines is plotted in Figure 6.2, along with the corresponding B_x sensitivity vectors for the points in Fig. 6.1. Clearly, the position sensitivity vector corresponds to the gradient vector at each point. Thus a complete set of iso-B_x curves, in the form of a contour map, would be an efficient means of visually identifying the magnetometer location with either high or low position sensitivity. Furthermore, since iso-B_x lines need not be drawn for fields lower than the ambient noise, this type of plot will also identify the zones where B_x can be measured with adequate signal to noise ratio.

The iso-B_y curves are shown in Fig. 6.3, with the obvious difference that B_y from an x dipole is zero on the coordinate axis while B_x is a maximum there. Figure 6.4 shows the iso-$|\vec{B}|$ curve, which can be seen to bound the curves for B_x and B_y. This figure shows that an instrument that measures $|\vec{B}|$ directly would have a much simpler position response than one measuring only a single component. It is also important to note that by the reciprocity theorem each of these iso-field curves can also be thought of as an iso-sensitivity curve for a magnetometer. This concludes the analysis of non-linear sensitivity vectors. Because of their straightforward interpretation, the iso-field plots and sensitivity vectors may be especially useful for studying the position sensitivity of quadrupole models.

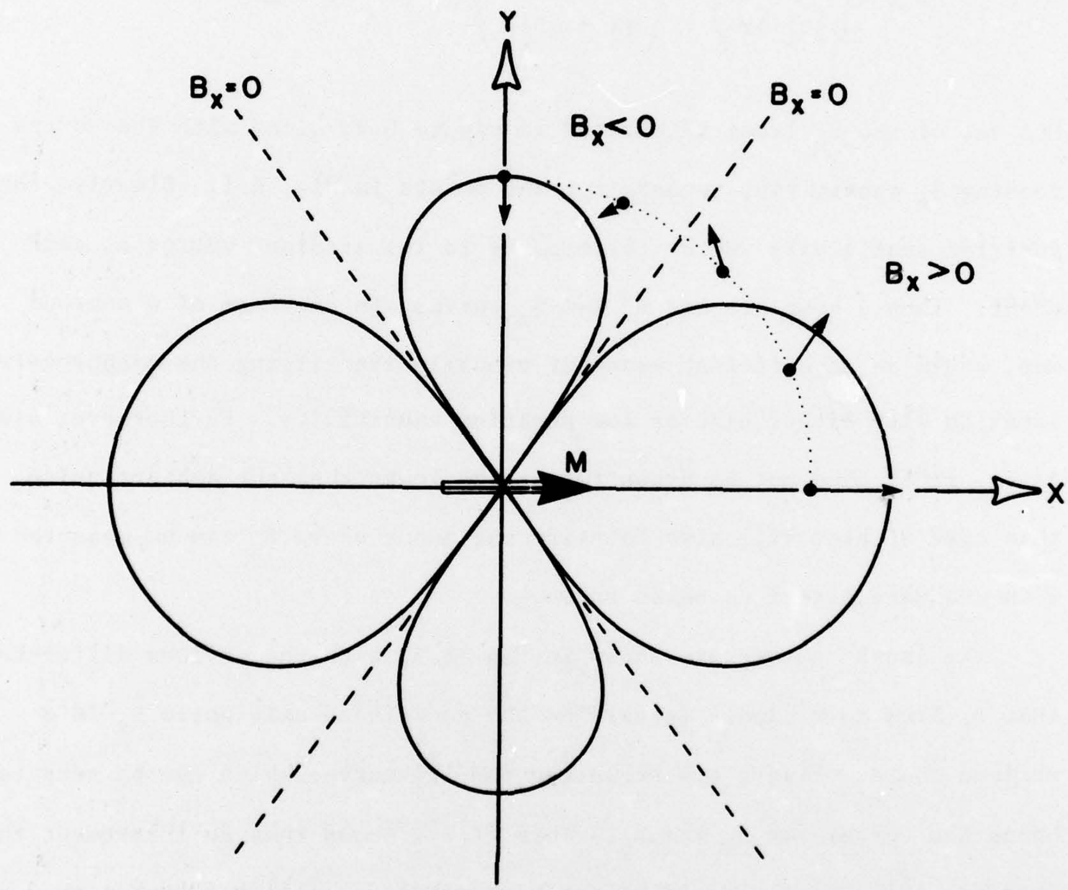

Fig. 6.2 The lines where $|B_x|$ produced by m_x is a constant.

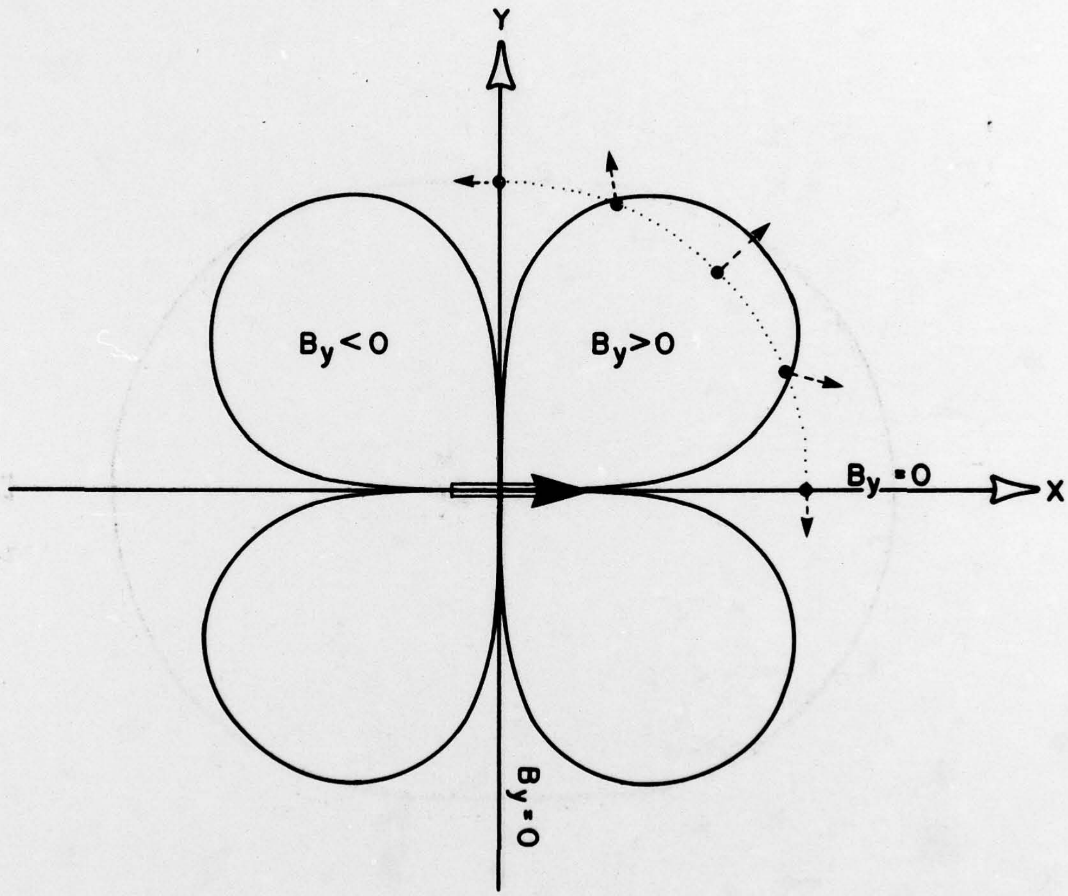

Fig. 6.3 The lines where $|B_y|$ produced by m_x is a constant.

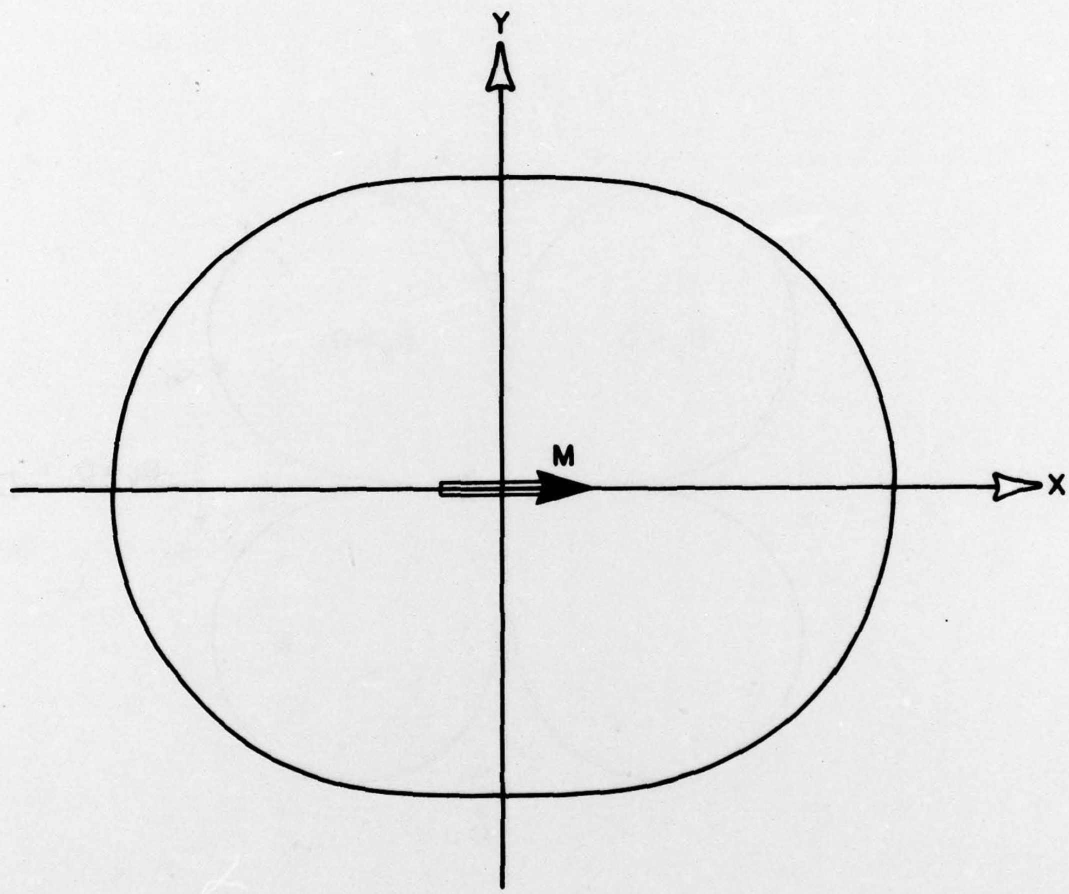

Fig. 6.4 The line where $|\vec{B}|$ from m_x is a constant.

VII. CONCLUSIONS

In this report, the mathematical basis of sensitivity vectors has been developed, with specific application to the measurement and modelling of magnetic fields. In the course of analyzing several examples, the following questions were answered:

1. Given two magnetic field measurements, what criteria must be satisfied to allow determination of the two dipole components consistent with that field?

2. For a measurement of the vector magnetic field at a fixed distance from a dipole source, what is the optimum magnetometer position?

3. How do various configurations of single axis magnetometers compare in terms of their ability to determine model parameters, and how can this be assessed quantitatively?

4. How can the presence of noise be included in such an analysis?

5. What is the relationship of the sensitivity vector concept to the reciprocity theorem of electromagnetic fields?

6. How can sensitivity vectors be used to study multipole models?

7. What is the interpretation of a sensitivity vector for a non-linear model?

8. What is the position dependence of a vector magnetometer, and how does it vary with position?

9. Where can a magnetometer be placed relative to the model to insure adequate signal to noise ratio?

Based on the ability of the sensitivity vector approach to answer these questions quantitatively, it appears that this type of analysis may be valuable for optimizing magnetometer array configurations. It is reassuring that the results obtained in this report are consistent with both a modeller's intuition and more abstract mathematical analysis, particularly in that this method can be readily extended to more complicated systems where intuition fails.

Two specific recommendations follow from this:

1) Interactive computer code should be developed to allow accurate and rapid analysis of magnetometer sensitivity and comparision of magnetometer configurations.

2) The sensitivity vector analysis should be extended to include the magnetic field from electric current distributions, and possibly the electric field from these currents.

In conclusion, sensitivity vectors are a potentially valuable technique that can be readily applied to the measuring and modelling of magnetic fields. Its greatest benefit over other techniques is that it allows simple, graphical display of magnetometer sensitivity.

ACKNOWLEDGEMENTS

The author is indebted to Darrel A. Nixon for his detailed comments and to John Breakwell for demonstrating the connection between sensitivity vectors and both the information matrix and the Taylor's series expansion of the source-field equation.

VIII. FIGURE CAPTIONS

Figure Captions (cont'd) Page

IX. LIST OF TABLES

List of Tables (cont'd)

X. LIST OF SYMBOLS

Symbols

$\vec{A}$	Magnetic vector potential
$\vec{B}$	Magnetic induction
$\vec{B}_p$	Magnetic induction from I_p in pickup coil
$\vec{E}$	Electric field
$\tilde{F}$, F_i	Scalar field measurement matrix
$\tilde{f}$	Non-linear functions of $\tilde{M}$
I_p	Test current
$\tilde{I}$	Identity matrix
$\hat{i}$, $\hat{j}$, $\hat{k}$, $\hat{e}_k$	Cartesian unit vectors
$\tilde{J}$	Jacobian matrix
$\tilde{M}$, M_i	Model matrix
$\vec{m}$, m_i	Magnetic dipole
$m \times 1$	Dimension of $\tilde{M}$
$n \times 1$	Dimension of $\tilde{F}$
$\lvert N_i \rvert$	Noise sensitivity vector
$\tilde{Q}$, Q_{ij}	Quadrupole Tensor
$\tilde{R}$	Information matrix
$\vec{r}$, $\vec{r}'$	Field and Source point distance vectors
$\tilde{S}_i$, $\vec{S}_i$, S_{i_x}	Sensitivity vector
$\tilde{T}$, T_{ij}	Transfer matrix
V	Model space volume

List of Symbols (cont'd)

Symbols

ω_i	Noise weighting function
α	Iso-field plot parameter
δ_{ij}	Kronecker Delta
ϕ	Magnetic flux
ϕ_i, ϕ_{ij}	Multipole unit potential
μ_o	Magnetic permeability of free space
∇	Gradient with respect to $\vec{r}$
∇'	Gradient with respect to $\vec{r}'$
∇_M	Gradient with respect to $\tilde{M}$

INITIAL DISTRIBUTION

Copies	
1	NRL (Code 5294) Mr. R. Clement
3	NUSC/NL 1 Code 343 (Mr. E. Soderberg) 1 Code 401 (Dr. R. Kasper) 1 Code 401 (Mr. J. Frye)
1	NCSC (Code 792) Dr. W. M. Wynn
5	NSWC/WOL 1 Code E22 (Mr. K. Bishop) 1 Code R43 (Mr. M. Kraichman) 1 Code E22 (Mr. M. Lackey) 1 Code R43 (Dr. R. Brown) 1 Code E22 (Mr. E. Peizer)
6	NAVSEA 1 SEA 05D 2 SEA 99612 3 PM2 (Mr. J. Crone Mr. Welsh CDR A. Cotterman)
1	Science Applications, Inc. Dr. J. Czika
30	Vanderbilt University Dr. J. Wikswo, Jr.
1	University of Pennsylvania Dr. R. Showers
12	DDC

CENTER DISTRIBUTION

Copies	Code
1	2704
5	2704, F. E. Baker
1	2731, S. H. Brown
2	2734, D. A. Nixon
1	2734, F. B. Walker
10	2734, B. R. Hood
1	522.2
2	5231

DTNSRDC ISSUES THREE TYPES OF REPORTS

1. DTNSRDC REPORTS, A FORMAL SERIES, CONTAIN INFORMATION OF PERMANENT TECHNICAL VALUE. THEY CARRY A CONSECUTIVE NUMERICAL IDENTIFICATION REGARDLESS OF THEIR CLASSIFICATION OR THE ORIGINATING DEPARTMENT.

2. DEPARTMENTAL REPORTS, A SEMIFORMAL SERIES, CONTAIN INFORMATION OF A PRELIMINARY, TEMPORARY, OR PROPRIETARY NATURE OR OF LIMITED INTEREST OR SIGNIFICANCE. THEY CARRY A DEPARTMENTAL ALPHANUMERICAL IDENTIFICATION.

3. TECHNICAL MEMORANDA, AN INFORMAL SERIES, CONTAIN TECHNICAL DOCUMENTATION OF LIMITED USE AND INTEREST. THEY ARE PRIMARILY WORKING PAPERS INTENDED FOR INTERNAL USE. THEY CARRY AN IDENTIFYING NUMBER WHICH INDICATES THEIR TYPE AND THE NUMERICAL CODE OF THE ORIGINATING DEPARTMENT. ANY DISTRIBUTION OUTSIDE DTNSRDC MUST BE APPROVED BY THE HEAD OF THE ORIGINATING DEPARTMENT ON A CASE-BY-CASE BASIS.